Synthesis, Antimalarial Activity, and Preclinical Pharmacology of a Novel Series of 4′-Fluoro and 4′-Chloro Analogues of Amodiaquine. Identification of a Suitable "Back-Up" Compound for *N-tert*-Butyl Isoquine

Paul M. O'Neill,*[†,‡] Alison E. Shone,[‡] Deborah Stanford,[†] Gemma Nixon,[†] Eghbaleh Asadollahy,[†] B. Kevin Park,[‡] James L. Maggs,[‡] Phil Roberts,[‡] Paul A. Stocks,[†] Giancarlo Biagini,[§] Patrick G. Bray,[§] Jill Davies,[§] Neil Berry,[†] Charlotte Hall,[§] Karen Rimmer,[§] Peter A. Winstanley,[‡] Stephen Hindley,[†] Ramesh B. Bambal,[ǁ] Charles B. Davis,[ǁ] Martin Bates,[⊥] Stephanie L. Gresham,[#] Richard A. Brigandi,[▽] Federico M. Gomez-de-las-Heras,[○] Domingo V. Gargallo,[○] Silvia Parapini,[¶] Livia Vivas,[◆] Hollie Lander,[◆] Donatella Taramelli,[¶] and Stephen A. Ward[§]

Department of Chemistry, University of Liverpool, Liverpool L69 7ZD, U.K., MRC Centre for Drug Safety Science, Department of Pharmacology and Therapeutics, School of Biomedical Sciences, University of Liverpool, Liverpool L69 3GE, U.K., Liverpool School of Tropical Medicine, Pembroke Place, Liverpool L3 5QA, U.K., Drug Metabolism and Pharmacokinetics, GlaxoSmithKline Drug Discovery, 1250 South Collegeville Road, Collegeville, Pennsylvania 19426, Medicines Research Centre, GlaxoSmithKline, Gunnels Wood Road, Stevenage, Hertfordshire SG1 2NY, U.K., Safety Assessment, GlaxoSmithKline, The Frythe, Welwyn, Hertfordshire AL6 9AR, U.K., Discovery Medicine Infectious Diseases CEDD, DDW DPU, GlaxoSmithKline, Upper Providence, Pennsylvania, GlaxoSmithKline, S.A., Parque Tecnológico de Madrid, Severo Ochoa, 2, 28760 Tres Cantos, Madrid, Spain, Dipartimento di Sanità Pubblica, Microbiologia, Virologia, Università degli Studi di Milano, Via Pascal, 36, 20133 Milan, Italy, and Department of Infectious and Tropical Diseases, London School of Hygiene and Tropical Medicine, Keppel Street, London WC1E 7HT, U.K.

On the basis of a mechanistic understanding of the toxicity of the 4-aminoquinoline amodiaquine (**1b**), three series of amodiaquine analogues have been prepared where the 4-aminophenol "metabolic alert" has been modified by replacement of the 4′-hydroxy group with a hydrogen, fluorine, or chlorine atom. Following antimalarial assessment and studies on mechanism of action, two candidates were selected for detailed ADME studies and in vitro and in vivo toxicological assessment. 4′-Fluoro-*N-tert*-butylamodiaquine (**2k**) was subsequently identified as a candidate for further development studies based on potent activity versus chloroquine-sensitive and resistant parasites, moderate to excellent oral bioavailability, low toxicity in in vitro studies, and an acceptable safety profile.

Introduction

Malaria is endemic in many of the poorest countries in the world, causing between 1–3 million deaths each year.[1,2] More than 90% of the deaths occur in sub-Saharan Africa, and nearly all the deaths are in children under the age of 5 years. The morbidity and mortality from malaria have been increasing over recent decades because of deterioration in health systems, growing drug[3] and insecticide resistance,[4] climate change, civil and social instability, and population displacement.[2]

The hemoglobin degradation pathway in *Plasmodium falciparum* has been successfully exploited as the therapeutic target of chloroquine (**1a**, Figure 1) and other 4-aminoquinolines.[5–7] As the parasite catabolizes human hemoglogin, the hematin biproduct (**1c**) is detoxified by crystallization to hemozoin. Chloroquine interacts with the porphyrin ring of the hematin by a π–π stacking interaction of the quinoline ring and accumulation of the heme/drug complex within the erythrocyte ultimately poisons the parasite.[8–10] Resistance to this mechanism
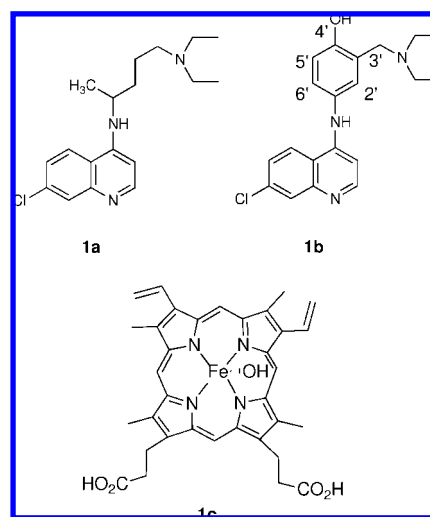

Figure 1. Structures of chloroquine (**1a**), amodiaquine (**1b**), and drug target hematin (**1c**).

of action has proven difficult to induce. Chloroquine resistance, which developed relatively slowly and only after considerable human exposure, is the result of point mutations in a parasite protein known as *Plasmodium falciparum* chloroquine resistance transporter (PfCRT[a]).[11]

* To whom correspondence should be addressed. Address: Department of Chemistry, University of Liverpool, Liverpool, L69 7ZD, UK. Phone: 0151-794-3553. Fax: XXXX. E-mail: p.m.oneill01@liv.ac.uk.

† Department of Chemistry, University of Liverpool.
‡ Department of Pharmacology and Therapeutics, University of Liverpool.
§ Liverpool School of Tropical Medicine.
ǁ GlaxoSmithKline Drug Discovery.
⊥ Medicines Research Centre, GlaxoSmithKline.
Safety Assessment, GlaxoSmithKline.
▽ Discovery Medicine Infectious Diseases CEDD, DDW DPU, GlaxoSmithKline.
○ GlaxoSmithKline, S.A., Spain.
¶ Università degli Studi di Milano.
◆ London School of Hygiene and Tropical Medicine.

[a] Abbreviations: ADME, absorption, distribution, metabolism, and excretion; PfCRT, *Plasmodium falciparum* chloroquine resistance transporter; GSK, GlaxoSmithKline; NOAEL, no observable adverse effect level; MNLD, maximum nonlethal dose; LAR, lipid accumulation ratio; VAR, vacuolar accumulation ratio.

Scheme 1. Oxidation of Amodiaquine to a Reactive Quinoneimine Metabolite
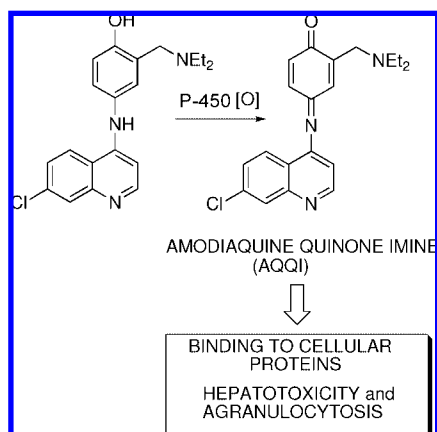
Amodiaquine (**1b**) is active against chloroquine-resistant strains of *P. falciparum*.[12] Until recently the use of this drug has somewhat been restricted by adverse effects in humans including hepatotoxicity and agranulocytosis.[13,14] This appears to be the result of bioactivation to form a reactive quinoneimine metabolite that binds irreversibly to cellular macromolecules and may lead to direct toxicity as well as immune-mediated hypersensitivity reactions (Scheme 1).[15−18] IgG antibodies have been detected in patients with adverse reactions to **1b**.[19,20]

In order to enhance the metabolic stability of amodiaquine, we demonstrated that introduction of fluorine into the 4-hydroxyanilino nucleus increases the oxidation potential of the molecule and reduces the in vivo oxidation of the molecule to a cytotoxic quinoneimine.[21] From this earlier work, we demonstrated that the 4′-hydroxyl group could be replaced with a 4′-fluorine atom to produce an amodiaquine analogue, fluoroamodiaquine (**2d**), with antimalarial activity in the low nanomolar range.[21]

An alternative approach to circumvent the facile oxidation of **1b** involves isomerization of the 3′ and 4′ groups. It was proposed that interchange of the 3′-hydroxyl and the 4′ Mannich side chain function of **1b** would provide a new series of analogues that cannot form toxic quinoneimine metabolites via cytochrome P450 mediated metabolism.[22] Isomeric amodiaquine analogues were prepared using a simple two-step procedure and then tested against K1 (chloroquine-resistant) and HB3 (chloroquine-sensitive) strains of *P. falciparum* in vitro.[22,23] While several analogues displayed potent antimalarial activity against both strains, isoquine (**1d**), the direct isomer of amodiaquine, was selected for in vivo antimalarial assessment. The potent in vitro antimalarial activity of **1d** was translated into excellent oral in vivo ED$_{50}$ activity of 1.6 and 3.7 mg/kg against the *P. yoelii* NS strain compared to 7.9 and 7.4 mg/kg for amodiaquine. Subsequent metabolism studies in the rat model demonstrated that isoquine does not undergo in vivo bioactivation, as evidenced by the complete lack of glutathione metabolites in bile. A drawback with **1d** is the low oral bioavailability in animal models, and this was demonstrated to be due to extensive metabolism of the *N*-diethylamino Mannich side chain. Further studies in this area have revealed that **1e** (Figure 2) has superior pharmacokinetic and pharmacodynamic profiles compared to isoquine in four animal species including primates. This compound has completed preclinical evaluation with Glaxo-SmithKline pharmaceuticals (GSK), and the phase I clinical trial commenced in April 2008.

The aim of this research was to investigate two series of amodiaquine analogues where the 4′-hydroxyl function of amodiaquine is replaced by either fluorine or chlorine; the intention, as in previous work, was to produce analogues incapable of producing quinoneimine metabolites by P450 oxidation. The array of target molecules is highlighted in Chart 1. For comparison purposes, we have also examined the antimalarial profile of two 4′-dehydroxy analogues of amodiaquine. Following completion of the syntheses and appropriate antimalarial assessment and preclinical pharmacological assessment, we aimed to select suitable back-up compounds to **1e** with appropriate properties suitable for drug development.

Chemistry

Although the original reported route to 4-fluoroamodiaquine was relatively efficient, we reasoned that shortening the number of synthetic steps and developing a route where a point of diversity appears in the penultimate step of the synthesis could achieve a significant improvement to the synthesis of target molecules in Chart 1. The alternative route adopted for the synthesis of 4′-chloro and 4′-fluoro analogues is shown in Scheme 2.

For the synthesis of 4′-chloro analogues, nitro reduction of **3a** was easily achieved using iron powder and HCl in refluxing aqueous ethanol. The resulting amine **3b** was then allowed to react with 4,7-dichloroquinoline to provide **3c** in excellent yield as a yellow powder following standard workup. Quinoline **3c** proved to be quite insoluble in dichloromethane, so a combination of dichloromethane, DMF, and a small amount of diisopropylethylamine was used as solvent to dissolve the alcohol for MnO$_2$ mediated oxidation. After 18 h of reflux, precipitates derived from the oxidant MnO$_2$ were filtered off. In many runs, significant losses occurred at this stage and a more satisfactory workup procedure involved the use of a precolumn with ethyl acetate prior to flash column chromatography using MeOH/dichloromethane as eluent. The key aldehyde was obtained in moderate to good yields following silica gel chromatography. The final step involved reductive amination of the aldehyde **13** with a variety of different amines to produce a small array of target molecules depicted in Chart 1. In all cases the reductive amination procedure worked well and column chromatography gave the products **3d−m** in good yields (Table 1).

Scheme 2 also depicts the synthesis of a fluorinated series of analogues, and the approach used is essentially the same as that discussed with the exception that alternative conditions were explored for the reduction of the nitro group of **2a** and the oxidation of the benzylic alcohol **2c** to the corresponding aldehyde. Disappointingly, the use of powdered iron/HCl gave the desired amine **3b** in low yields following basification and workup. Alternative reducing conditions using methanol, ammonium chloride, and zinc powder or granulated tin and concentrated hydrochloric acid provided the product in good yield following addition of sodium hydroxide solution to the amine in the workup phase of the reaction. The synthesis of **2b** from **2c** proceeded in high yields without event. In contrast to the 4′-chloro series, oxidation of **2c** with MnO$_2$ gave the desired aldehyde in poor yields, possibly because of the insolubility of the quinoline aldehyde. An alternative method based on chromium(VI) was explored that provided the aldehyde in moderate yield. Reductive amination and workup provided the desired compounds as a dark-brown solid. NMR analysis of the products prior to chromatography indicated complex formation (very broad peaks in the aromatic and aliphatic regions), the nature of which remains undefined. Acidification (HCl) and basification (sodium bicarbonate) provided the free bases which were pure by NMR and CHN analysis following silica gel column
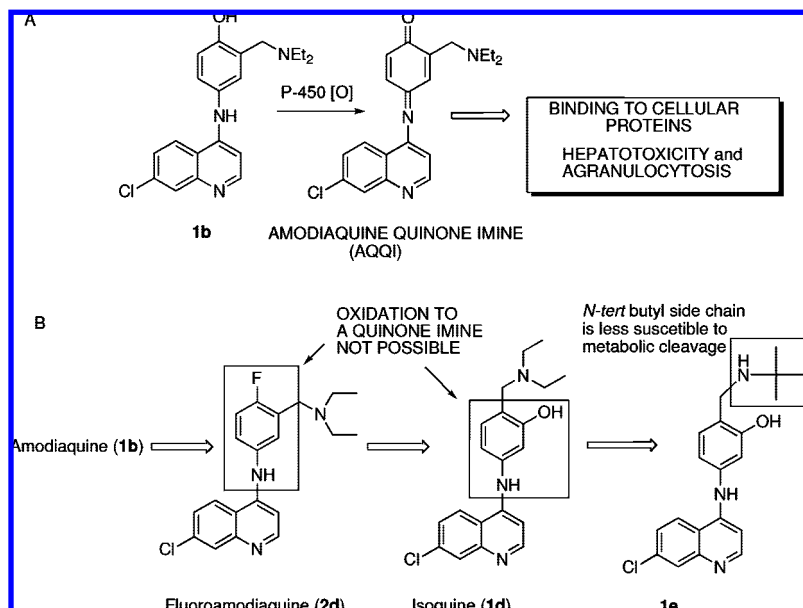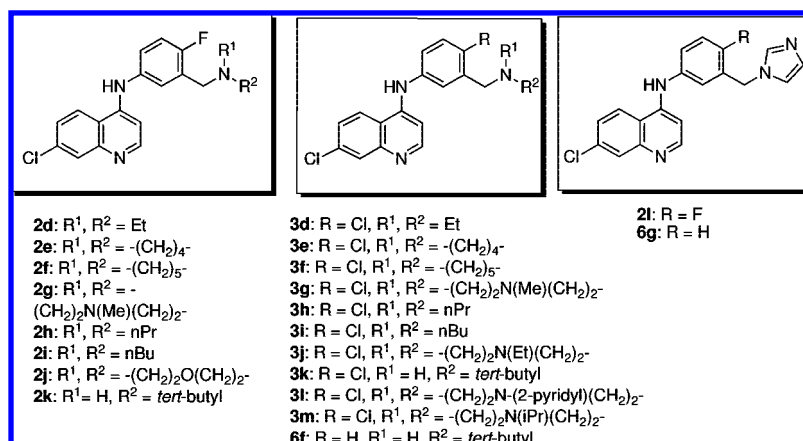
Figure 2. Rational drug design of amodiaquine analogues based on metabolism/toxicity considerations. Clinical candidate **1e** has an exceptional pharmacodynamic and pharmacokinetic profile.

Chart 1. Structures of 4′-Chloro and 4′-Fluoro Analogues of Amodiaquine

2d: R^1, R^2 = Et
2e: R^1, R^2 = -(CH$_2$)$_4$-
2f: R^1, R^2 = -(CH$_2$)$_5$-
2g: R^1, R^2 = -(CH$_2$)$_2$N(Me)(CH$_2$)$_2$-
2h: R^1, R^2 = nPr
2i: R^1, R^2 = nBu
2j: R^1, R^2 = -(CH$_2$)$_2$O(CH$_2$)$_2$-
2k: R^1 = H, R^2 = *tert*-butyl

3d: R = Cl, R^1, R^2 = Et
3e: R = Cl, R^1, R^2 = -(CH$_2$)$_4$-
3f: R = Cl, R^1, R^2 = -(CH$_2$)$_5$-
3g: R = Cl, R^1, R^2 = -(CH$_2$)$_2$N(Me)(CH$_2$)$_2$-
3h: R = Cl, R^1, R^2 = nPr
3i: R = Cl, R^1, R^2 = nBu
3j: R = Cl, R^1, R^2 = -(CH$_2$)$_2$N(Et)(CH$_2$)$_2$-
3k: R = Cl, R^1 = H, R^2 = *tert*-butyl
3l: R = Cl, R^1, R^2 = -(CH$_2$)$_2$N-(2-pyridyl)(CH$_2$)$_2$-
3m: R = Cl, R^1, R^2 = -(CH$_2$)$_2$N(iPr)(CH$_2$)$_2$-
6f: R = H, R^1 = H, R^2 = *tert*-butyl

2l: R = F
6g: R = H

Scheme 2. Synthesis of 4′-Fluoro and 4′-Chloro Analogues by Reductive Amination of Aldehydes **2c** and **3c**[a]

2a: R = F
3a: R = Cl

2b: R = F
3b: R = Cl

2c: R = F
3c: R = Cl

**2d-2j**: R = F
3d-3m: R = Cl
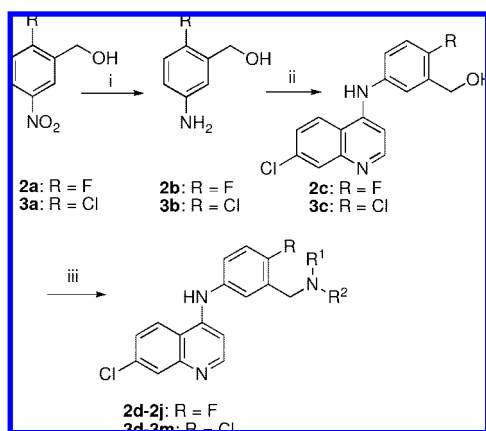
[a] Reagents and conditions (i) Fe/HCl/H$_2$O, reflux; (ii) 4,7-dichloroquinoline, EtOH, reflux; (iii) DIEA, CH$_2$Cl$_2$, DMF, MnO$_2$; (iv) amine, then NaHB(OAc)$_3$.

Table 1. Yields for Reductive Amination of Aldehydes **2c** and **3c**

aldehyde	amine	product	yield (%)
	Fluoro Series		
2c	diethylamine	**2d**	24
2c	pyrrolidine	**2e**	20
2c	piperidine	**2f**	31
2c	*N*-methylpiperazine	**2g**	31
2c	dipropylamine	**2h**	27
2c	dibutylamine	**2i**	42
2c	morpholine	**2j**	23
	Chloro Series		
3c	diethylamine	**3d**	74
3c	pyrrolidine	**3e**	61
3c	piperidine	**3f**	92
3c	*N*-methylpiperazine	**3g**	89
3c	dipropylamine	**3h**	85
3c	dibutylamine	**3i**	24
3c	*N*-ethylpiperazine	**3j**	63
3c	*tert*-butylamine	**3k**	59
3c	1-(2-pyridyl)-piperazine	**3l**	98
3c	*N*-isopropylpiperazine	**3m**	56

chromatography. Although the new route examined provided target molecules in acceptable yields for the 4′-chloro series,

the final reductive amination step in the 4′-fluoro series requires optimization (Table 1).

Scheme 3. Synthesis of 4-Dehydroxy, 4′- Chloro, and 4′-Fluoro Analogues of Amodiaquine[a]
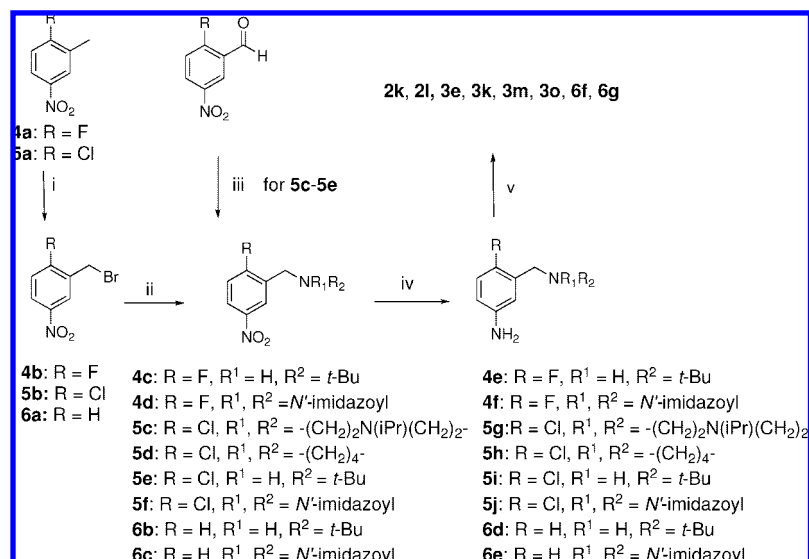
a Reagents and conditions: (i) NBS, AIBN, reflux; (ii) amine, K_2CO_3, CH_3CN, reflux; (iii) MeOH, room temp, then 0 °C, $NaHB(OAc)_3$; (iv) Sn/HCl, H_2O, reflux; (v) 4,7-dichloroquinoline, EtOH, HCl, reflux.

Table 2. In Vitro Antimalarial Activities[24] versus Chloroquine Sensitive 3D7 Strain of *Plasmodium falciparum*[a]

compd[b]	IC$_{50}$ (nM) 3D7	compd[b]	IC$_{50}$ (nM) 3D7
2d	27.3 (3) ± 11.5	**3d**	30.4 (3) ± 15.2
2e	29.7 (3) ± 11.1	**3f**	25.7 (3) ± 10.6
2f	33.2 (3) ± 15.2	**3g**	86.8 (3) ± 43.1
2g	35.1 (3) ± 8.7	**3h**	277.3 (3) ± 34.6
2h	85.2 (3) ± 18.1	**3i**	345.2 (3) ± 9.3
2i	95.2 (3) ± 30.2	**3j**	39.7 (3) ± 9.3
2j	550.7 (3) ± 90.4	**3k**	7.8 (6) ± 3.2
2k	12.1 (3) ± 5.3	**3l**	27.2 (3) ± 18.1
2l	27.2 (3) ± 3.4	amodiaquine (**1b**)	4.7 (3) ± 2.9
chloroquine (**1a**)	9.1 (3) ± 4.9	**1e**	6.0 (6) ± 4.0
isoquine (**1d**)	7.8 (6) ± 2.2		

a 3D7 is a chloroquine sensitive strain of *P. falciparum*. *b* Amodiaquine and **1e** were tested as the hydrochloride salt. Chloroquine was tested as the diphosphate. All other compounds were tested as free bases.

Table 3. In Vitro Antimalarial Activities[24] of 4-Chloro Series versus Chloroquine-Sensitive HB3 Strain and TM6 Chloroquine-Resistant *Plasmodium falciparum*[a]

	IC$_{50}$ (nM)	
compd	TM6	HB3
3d	10.2 ± 5.3	12.3 ± 5.1
3e	4.2 ± 1.3	15.2 ± 3.7
3f	9.4 ± 6.7	12.3 ± 3.2
3g	24.4 ± 4.8	54.5 ± 8.3
3i	96.3 ± 11.3	144.3 ± 12.8
3j	10.3 ± 4.3	9.6 ± 3.4
3k	4.5 ± 3.2	8.1 ± 3.2
3l	500 ± 22.4	485 ± 14.1
3m	6.4 ± 2.3	9.1 ± 2.1
4d	5.0 ± 2.2	10.1 ± 3.2
chloroquine (**1a**)	95.1 ± 6.5	20.2 ± 10.1
amodiaquine (**1b**)	7.2 ± 3.3	5.5 ± 3.2

a TM6 is a chloroquine resistant strain of *P. falciparum*, and HB3 is a chloroquine sensitive strain of *P. falciparum*.

For this reason, the previously used linear approach was employed for selected analogues as shown Scheme 3. The first step in the sequence involved free radical bromination of 2-fluoro-5-nitrotoluene (or 2-chloro-5-nitrotoluene) using NBS/AIBN to give the benzylic bromide **4b** as a crystalline solid in good yield. The resulting benzyl bromide **4b** was then allowed to react with the appropriate amine to provide intermediates (**4c**, **4d**, **5c–f**, **6b**, and **6c**) that were reduced and coupled with 4,7-dichloroquinoline as shown. Benzyl bromides **4b**, **5b**, and **6a** were also allowed to react with imidazole, and this enabled the synthesis of novel weak base imidazole derivatives **2l**, **3p**, and **6g**. For intermediates **5c–e**, 2-chloro-5-nitrobenzaldehyde was also used as starting material in a reductive amination approach as shown.

Biology

In Vitro Antimalarial Activity versus *Plasmodium falciparum*.[24,25] Initial testing[24] was carried out on a chloroquine-resistant strain of *Plasmodium falciparum* (3D7) (Table 2). In the 4′-fluoro series the weak base morpholine analogue **2j** and analogues **2h** and **2i** expressed relatively poor antimalarial activity versus the 3D7 strain. The former observation has been seen previously with short chain analogues of chloroquine;[26] for **2h** and **2i** it would appear that increasing the lipophilicity has a detrimental effect on antimalarial activity (ClogP for **2h**

and **2i** of >5.89). The *N-tert*-butyl analogue **2k** (log P = 4.74) was the most potent in this series with activity equivalent to that of chloroquine and isoquine (**1d**). The 4′-chloro analogues tested were all active around 30 nM with the exception of dipropyl and dibutyl analogues **3g** and **3h**, and in line with the 4′-fluoro series, the 4′-chloro-*N-tert*-butyl analogue **3k** expressed the highest antimalarial activity. Interestingly, within these two templates, the side chain alkylamine or cyclic amine groups can be replaced with imidazole to produce analogues **2l** and **3p** that had antimalarial activity in the low nanomolar range.[27]

Table 3 lists activity for the 4′-chloro series versus a chloroquine-resistant TM6 and sensitive HB3 strain. The most potent analogue was the *N-tert*-butyl analogue **3k**. Analogues **3e**, **3f**, **3j**, and **3m** also expressed excellent activities against these two strains. For the series as a whole there is a clear lack of cross-resistance for the 4′-chloro series. The replacement of the 4′-F or 4′-Cl with hydrogen coupled with *N-tert*-butyl substitution provides (**6f**) an analogue with equipotent activity against the HB3 and TM6 strains of *Plasmodium falciparum*. Despite the good activity of this molecule, it was not selected for in vivo evaluation because of the concerns that metabolically 4-hydroxyanilino ring system may be susceptible to P450

Table 4. Expanded in Vitro Antimalarial Activities[24] of **2e** and **2k** versus a Panel of *Plasmodium falciparum* Isolates[a]

strain	chloroquine (**1a**)	amodiaquine (**1b**)	**2e**	**2k**
	IC_{50} (nM)			
TM6	112.0 ± 15.3	6.91 ± 3.2	60.8 ± 8.9	21.9 ± 5.4
K1	170.6 ± 22.3	20.0 ± 2.3	45.9 ± 12.2	22.0 ± 3.4
HB3	16.0 ± 3.4	8.5 ± 3.4	63.7 ± 11.2	14.6 ± 5.4
PH3	30.8 ± 12.3	15.21 ± 4.4	25.0 ± 8.2	25.8 ± 6.7
TM4	112.8 ± 22.2	15.1 ± 3.3	46.9 ± 18.1	17.3 ± 4.9
DD2	59.3 ± 11.1	9.5 ± 1.4	36.9 ± 4.9	22.4 ± 1.6
V1S	154.0 ± 17.3	8.9 ± 4.6	52.5 ± 9.5	26.1 ± 7.6
J164	133.5 ± 14.5	18.5 ± 4.2	34.7 ± 8.3	29.24 ± 4.5

[a] TM6, K1, TM4, V1S, J164 are all chloroquine-resistant strains of *P. falciparum*. The rest of the strains are chloroquine-sensitive.

Table 5. Therapeutic Efficacy of **2k**, **2m**, Isoquine, and Desethylisoquine against *Plasmodium berghei* ANKA Infection in Mice Using the Standard 4-Day Test Assay[a]

compd	ED_{50} (mg/kg)	95% confidence interval	ED_{90} (mg/kg)	95% confidence interval
amodiaquine (**1b**)	2.1	2.0−2.2	3.2	2.9−3.4
isoquine (**1d**)	3.7	3.4−3.9	5.3	4.3−6.6
desethyl isoquine (**1f**)	5.3	4.1−6.8	7.3	6.4−8.4
2k	5.3	4.1−6.8	12.4	10.7−14.4
3k	13.4	11.2−15.6	27.3	14.3−30.2

[a] Groups of five mice were inoculated iv with 10^7 infected erythrocytes/mice. The compound was administered orally once a day for 4 days starting 1 h after infection. Seven drug doses were used ranging from 40 to 0.31 mg/kg to determine ED_{50} and ED_{90} values. Parasitemia after treatment was measured in peripheral blood by flow cytometry 24 h after the administration of the fourth dose.

mediated hydroxylation that would produce 4-aminophenol or 2-aminophenol quinoneimine precursors.

As this project progressed, the excellent profiles displayed by the isoquine analogue **1d** and in particular the metabolic advantages provided by the *N-tert*-butyl side chain seen in the development of **1e** led to the selection of **2k** for further expanded biological assessment against eight additional strains of *Plasmodium falciparum*. In the expanded testing contained in Table 4, data are also included for the pyrollidine analogue **2e**.

The data indicate that **2k** is superior to the additional control analogue **2e** against all of the strains examined. It is also clear that *N-tert*-butyl analogue **2k** is potent against chloroquine resistant strains, though it is not quite as active as amodiaquine against both chloroquine-sensitive and resistant parasites. On the basis of the activity presented in Table 4, **2k** was selected alongside its direct 4-chloro analogue for further studies in the mouse model of malaria.

In Vivo Antimalarial Activity against *Plasmodium berghei* ANKA.[28] The therapeutic efficacy of **2k**, **3k**, and selected 4-aminoquinolines was evaluated in a standard "4-day test" in CD1 mice infected intravenously with the murine pathogen *P berghei* ANKA at GSK, Tres Cantos, Spain (Table 5).

Isoquine (**1d**) showed in vivo therapeutic efficacy against *Plasmodium berghei* ANKA with ED_{50} and ED_{90} in the same range as that of amodiaquine. Analogue **2k** was also potent in this in vivo assay with an ED_{50} value of 5.3 mg/kg, whereas chloro analogue **3k** was less potent with an ED_{50} of 13.4 mg/kg. The therapeutic efficacy of **2k**, isoquine (**1d**), **1f**, and the two control compounds amodiaquine and chloroquine were also evaluated in the standard "4-day test" against the murine pathogen *P. yoelii* 17X. Mice were infected with 6.4×10^6 parasitized erythrocytes/mouse iv. Treatments started 1 h after infection, and each drug was administered once a day po in saline. Parasitemias in peripheral blood were measured 96 h after infection (day 4) and then every 2−3 days until day 23

Table 6. Therapeutic Efficacy of **2k** and Isoquine Derivatives against *Plasmodium yoelii* 17X Infection in Mice[a]

compd	test	parameter	mean (mg/kg)	IC 95%[b] (mg/kg)
chloroquine (**1a**)	4-day	ED_{50}[c]	3.3	2.8−3.7
		ED_{90}	4.4	4.0−4.9
		NRL[d]	>40[e]	NA[f]
amodiaquine (**1b**)	4-day	ED_{50}	2.6	2.1−3.2
		ED_{90}	3.7	3.3−4.1
		NRL	>40[e]	NA[f]
isoquine (**1d**)	4-day	ED_{50}	5.2	4.6−5.8
		ED_{90}	7.6	6.9−8.3
		NRL	>40[e]	NA[f]
desethylisoquine (**1f**)	4-day	ED_{50}	5.5	5.1−5.9
		ED_{90}	8.0	7.6−8.5
		NRL	>40[e]	NA[f]
2k	4-day	ED_{50}	7.7	6.7−8.9
		ED_{90}	10.6	9.4−11.8
		NRL	>40[e]	NA[f]

[a] Standard 4-day test assay. Chloroquine and amodiaquine were included as control compounds.[28] [b] Interval of confidence of the mean. [c] Dose at which a 50% of reduction of parasitemia in peripheral blood is achieved at day 4 after infection. [d] Nonrecrudescence level (NRL) is defined as the minimum dose at which no recrudescence is observed. Highest dose deployed in this study was 40 mg/kg. [e] NRL level is only defined for treatments that make parasitemia undetectable by flow cytometry at day 4 in the "4-day test". At the highest dose deployed chloroquine, amodiaquine, isoquine, desethylisoquine, and **2k** (40 mg/kg) were unable to render parasitemia undetectable; therefore, it is not possible to evaluate NRL level for these compounds accurately. It is higher than 40 mg/kg. [f] NA = not applicable.

Scheme 4. Potential Binding Interactions for Drug (**L**) with Heme (**P**)[a]
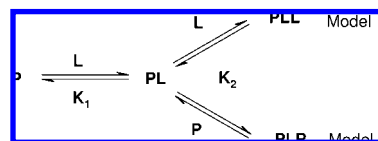
[a] After the first association of porphyrin with drug, there are two distinct binding events in which either another drug or porphyrin molecule coordinate to the intermediate adduct.

after infection in order to assess recrudescence after treatment. The results (ED_{50}, ED_{90}, and nonrecrudescence level) are shown in Table 6.

Mechanism of Action. Hematin Binding Studies. Recent efforts have centered on developing titration methods to determine accurate equilibrium constants and binding stoichiometries for the most widely used quinoline antimalarials.[29−36] We have applied a UV−visible spectroscopic method for determining accurate binding equilibrium constants for several clinically used antimalarials and compared the results with fluoro analogue **2k**. Initially, the titrations were carried out in a mixed aqueous/organic solvent to minimize porphyrin aggregation effects and μ-oxo-dimer formation. Buffered 40% DMSO was used to provide a strictly monomeric heme species in solution.[35]

The mode of action for antimalarial binding was investigated. The potential binding processes 1 and 2 shown in Scheme 4 were mathematically modeled and examined as possible best fits for the titrations. In model 1 there is a stepwise bonding of 2 equiv of drug to 1 molecule of heme. In model 2 there is a stepwise addition of 2 additions of heme to 1 equiv of drug.

The UV−visible spectra obtained after each titrated addition were analyzed and stacked against the corresponding absorbances. The data were transferred for analysis using the Pro-Fit nonlinear curve fitting program licensed from Quansoft. The data were fitted to achieve χ^2 at a minima to produce K_1 and K_2 fitted parameters for both models. This was initially done at

Table 7. Equilibrium Constants for the Binding of Antimalarials with Heme in DMSO Solutions

compound	solvent	$\log K_1$	$\log K_2$	best fit model
chloroquine (**1a**)	40% DMSO	4.60 ± 0.1	6.70 ± 0.1	2
amodiaquine (**1b**)	40% DMSO	4.40 ± 0.1	6.20 ± 0.1	2
quinine	40% DMSO	4.40 ± 0.1	4.10 ± 0.1	1
mefloquine	40% DMSO	3.84 ± 0.1	3.17 ± 0.1	1
2k	40% DMSO	5.45 ± 0.1	5.68 ± 0.1	2

Table 8. Results of the β Hematin Inhibition Assay (BHIA) Assay[37]

compd	$IC_{50}{}^a$ molar ratio for drug/hemin
2k	1.66
2l	1.78
3k	1.66
3p[b]	1.58
3m	1.66
6f	1.65
6g	2.65
chloroquine (**1a**)	1.78
amodiaquine (**1b**)	0.85

^a The IC_{50} represents the molar equivalents of test compounds, relative to hematin, required to inhibit β-hematin formation. ^b Compound not completely dissolved.

one wavelength and then simultaneously at $10-15$ wavelengths to give a more unbiased approach to fitting and more accurate values in comparison to fitting at just a single wavelength. Table 7 above shows the K_1 and K_2 values obtained from this method for chloroquine, amodiaquine, quinine, **2k**, and mefloquine, with the best fitted model shown.

An important observation indicated from the resulting fits is that the binding stoichiometries for the quinoline methanols quinine and mefloquine are different from the 4-aminoquinolines included in this work; the second binding event in the chloroquine titrations involves the addition of another molecule of heme, whereas the second binding to the quinine−heme adduct involves a second molecule of ligand. This is in line with earlier studies derived from NMR experiments suggesting that the binding modes of 4-aminoquinoline antimalarials, such as chloroquine and amodiaquine, and quinolinemethanol antimalarials, such as quinine and mefloquine, are different.[35,36]

The data measured are in good agreement with the literature and demonstrate that the fluoro analogue **2k** can form a 2:1 complex in solution with clearly defined association constants. Selected analogues from the new series of 4-aminoquinolines were also examined for their ability to inhibit β-hematin formation using the method of Parapini et al.[37]

The drug concentration required to inhibit β-hematin formation by 50% (IC_{50}) was determined for each compound, and the results listed in Table 8 are the mean IC_{50} of two different experiments performed in duplicate. All of the compounds tested had excellent activity in this assay including the imidazole containing analogues **2l**, **3p**, and **6g**. These molecules are interesting in the sense that in addition to $\pi-\pi$-stacking over the porphyrin ring system of hematin these agents may have the capacity to interfere with hematin dimerization or crystallization by binding to iron by axial ligation.[27] Both **2k** and chloro variant **3k** had superimposible activity in the assay.

Disposition and Metabolism Studies. In order to determine the effect of replacing the 4′-hydroxy group in the amodiaquine-like framework with fluorine and chlorine atoms, distribution and metabolism studies were carried out in the rat. The requisite [³H] labeled 4′-fluoro derivative **2k** and 4′-chloro analogue **3k** were prepared by the route depicted in Scheme 2, and further details are available in the Supporting Information. Five hours

after administration of a single dose of [³H]**2k** to cannulated rats $55.94 \pm 5.82\%$ of the dose could be accounted for in the organs, bile, and urine (Figure 3). The pattern of distribution followed that seen previously following metabolism of other 4-aminoquinolines such as amodiaquine and chloroquine, with the majority of the dose being retained in the liver ($17.49 \pm 0.82\%$) and skin ($12.44 \pm 1.76\%$). Elimination of the drug seemed to be favored by neither biliary nor urinary excretion systems, with $9.16 \pm 1.29\%$ of the dose being excreted in bile and $8.06 \pm 1.12\%$ being excreted in the urine.

As might be expected, the pattern of distribution of [³H]**3k** in the tissues of male Wistar rats followed the same pattern as the other 4-aminoquinoline compounds tested. Slightly less radioactivity than **2k** was recovered in the tissues, bile, and urine, $47.35 \pm 4.77\%$, the majority of which could be found in the liver ($12.41 \pm 0.29\%$). Significant differences in areas of accumulation were seen with the kidneys, liver, biliary, and urinary output. Five hours after dosing with [³H]**3k** there was significantly more radioactivity found in the kidneys than observed with [³H]**2k**, $5.43 \pm 0.28\%$ versus $3.97 \pm 0.13\%$ ($p = 0.0054$). In the liver, there was significantly less [³H]**3k** than [³H]**2k** ($p = 0.0209$). This was followed by a significant increase in biliary excretion after dosing with [³H]**3k** ($14.88 \pm 0.83\%$, $p = 0.0052$). The increased biliary excretion of **3k** compared to **2k** could be attributed to increased lipophilicity ($\log P = 5.59 \pm 0.51$ versus $\log P = 5.15 \pm 0.56$).

On comparison of the tissue distribution of the two novel compounds with amodiaquine (**1b**), 5 h after administration it can be observed that at an equivalent dose, the halogenated analogues appear to accumulate in the major organs to a much lesser extent than amodiaquine (Figure 4). In the brain, kidneys, liver, and skin it can be seen that there was significantly less retention with the halogenated analogues of **1b**.

Animals were dosed with either [³H]**2k** or [³H]**3k** and kept in metabolism cages for a period of 24 h in order to see if the drugs were effectively eliminated or if they would accumulate in the tissues over time (Figure 5). Results showed that both drugs were effectively eliminated after 24 h, with the total amount of radioactivity recovered with [³H]**2k** and [³H]**3k** being $51.36 \pm 8.68\%$ and $61.00 \pm 5.93\%$, respectively. In the kidneys, almost 2-fold more drug was found in rats dosed with [³H]**2k** than those dosed with [³H]**3k**, $1.48 \pm 0.11\%$ versus $0.31 \pm 0.07\%$; this was found to be highly significant ($p < 0.0001$). The same was observed on comparison of the radioactivity retained in the liver 24 h after dosing. After dosing with [³H]**2k**, $6.57 \pm 0.27\%$ of the dose remained in the liver, while after dosing with the chloro analogue only $1.87 \pm 0.21\%$ remained (3.5-fold less). This showed mathematical significance with $p < 0.0001$. The lungs were another example where the choice of halogen substitute appeared to make a great difference to the retention of the drug. After dosing with [³H]**2k**, $1.17 \pm 0.06\%$ of the dose remained. In comparison, after dosing with [³H]**3k**, only $0.25 \pm 0.08\%$ remained, a decrease of almost 5-fold ($p < 0.0001$).

Although the amount of [³H]**2k** remaining in the rat after 24 h was relatively low (14.76 ± 2.47) (compared to $38.54 \pm 3.41\%$ after 5 h) and significantly lower in the liver and skin ($p = 0.0286$ and $p = 0.0011$, respectively), it was deemed appropriate to investigate to further time points (Figure 6). After 48 h $72.79 \pm 2.56\%$ of the dose could be accounted for in tissues, feces, and urine. Of this, less than 8% remained in the tissues; the remainder had been excreted, mainly by biliary excretion. After 1 week (168 h) very little radioactivity remained inside the rat ($1.22 \pm 0.24\%$). After 10 days (240 h) radioactivity
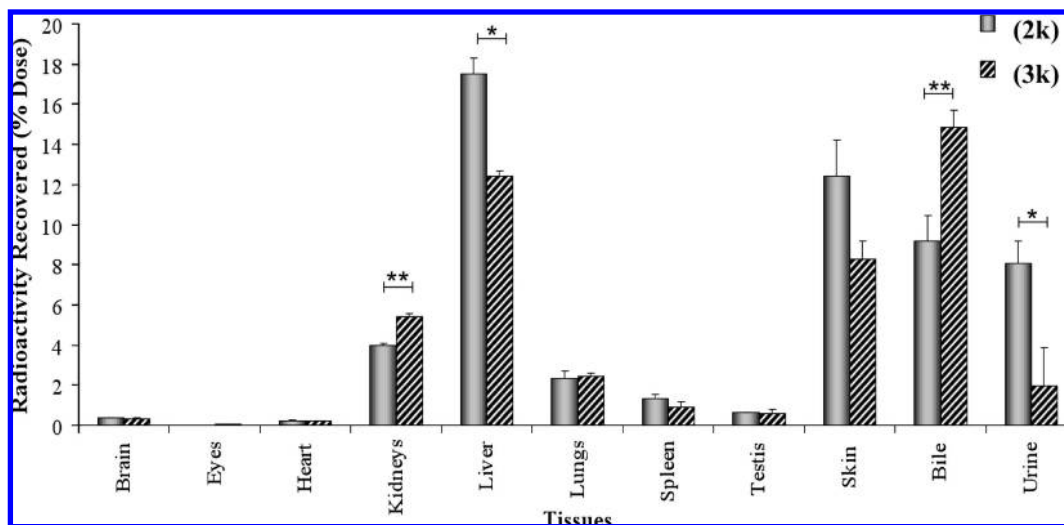
Figure 3. Percentage of radioactive dose recovered in tissues 5 h after administration of [³H]**2k** and [³H]**3k** (54 μmol/kg, 20 μCi/rat) to male Wistar rats ($n = 4$). Results are expressed as mean percentage of dose ± SEM. Statistics were performed using a one-way ANOVA test for parametric data and Kruskal−Wallis test for nonparametric data: (*) $P < 0.05$; (**) $P < 0.01$; (***) $P < 0.001$.
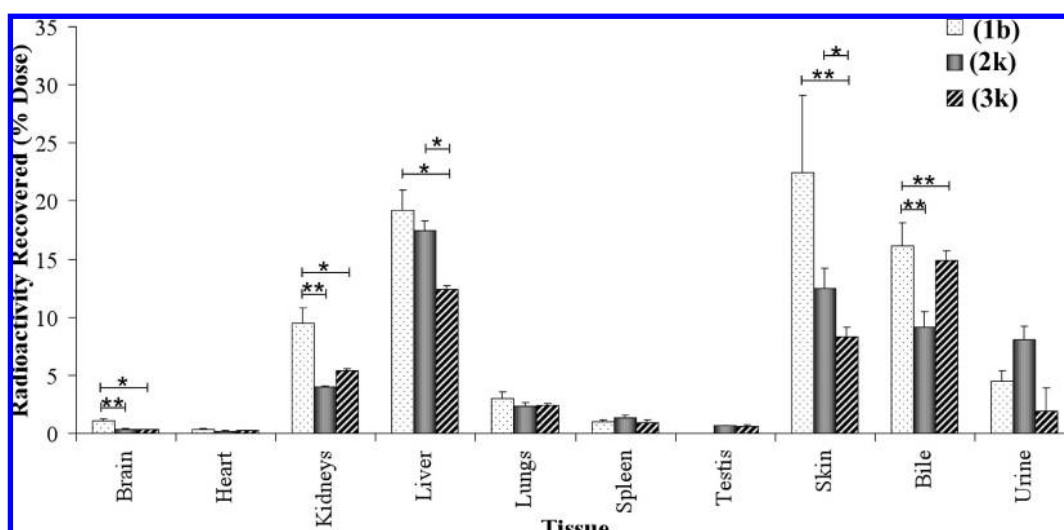

Figure 4. Percentage of radioactive dose recovered in tissues 5 h after administration of [³H]amodiaquine, [³H]**2k**, and [³H]**3k** (54 μmol/kg, 20 μCi/rat) to male Wistar rats ($n = 4$). Results are expressed as mean percentage of dose ± SEM. Statistics were performed using a one-way ANOVA test for parametric data and Kruskal−Wallis test for nonparametric data: (*) $P < 0.05$; (**) $P < 0.01$; (***) $P < 0.001$.

was negligible in the tissues of the rat, indicating a lack of accumulation and the effective clearance of [³H]**2k** after a single dose of 54 μmol/kg.

From these dispositional in vivo studies it is clear that both **2k** and **3k** show a similar pattern of distribution to other 4-aminoquinolines of the same class, with the majority of the dose being found in the liver and skin. Incorporation of a halogen appears to reduce the retention within the tissues compared to **1b**; however, the choice of halogen is important because the chloro analogue appears to have significantly less retention and was cleared much more effectively by biliary excretion. After studies have been carried out for up to 10 days, it has been shown that [³H]**2k** was effectively cleared from the rat and there were no issues of irreversible retention.

Metabolism Studies on 2k and 3k. Following administration of [³H]**2k** (54 μmol/kg, 20 μCi) to male Wistar rats, a total of nine metabolites were found in bile and urine in rats in vivo (Table 9). Of these, four have been identified and the structures elucidated (Scheme 5). (For full methods of analysis and protocols, see Supporting Information.) The

major biliary metabolite of [³H]**2k** was shown to yield *m/z* 469; however, a corresponding structure could not be assigned. In urine [³H]**2k** was excreted mainly as the parent compound. There was no evidence for P450 hydroxylation of the 4′-fluoro aromatic ring to produce aminophenol metabolites capable of reactive metabolite generation. This was further backed up by the observation that no glutathione conjugates were identified indicating that the incorporation of fluorine into the amodiaquine backbone has eliminated the possibility of the formation of toxic quinoneimine metabolites.

Metabolism studies on [³H]**3k** were carried out in male Wistar rats (54 μmol/kg, 20 μCi, iv). All major metabolites were structurally assigned (Scheme 6, Table 10). The major route of metabolism appeared to be oxidation to the side chain carboxylic acid **IV** (Scheme 6). Oxygenation of the nitrogen of the quinoline ring to form the *N*-oxide **III** was also observed. No evidence of P450 hydroxylation of the 4′-chloro ring system was obtained and no bioactivation to reactive
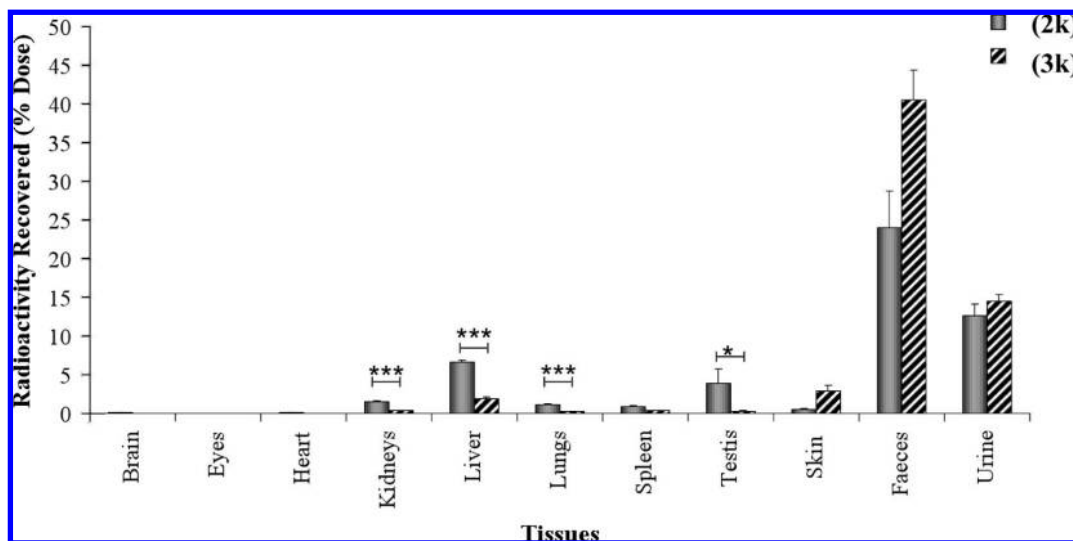
Figure 5. Percentage of radioactive dose recovered in tissues 24 h after administration of [^{3}H]**2k** and [^{3}H]**3k** (54 μmol/kg, 20 μCi/rat) to male Wistar rats ($n = 4$). Results are expressed as mean percentage of dose $\pm$ SEM. Statistics were performed using a one-way ANOVA test for parametric data and Kruskal–Wallis test for nonparametric data: (*) $P < 0.05$; (**) $P < 0.01$; (***) $P < 0.001$.
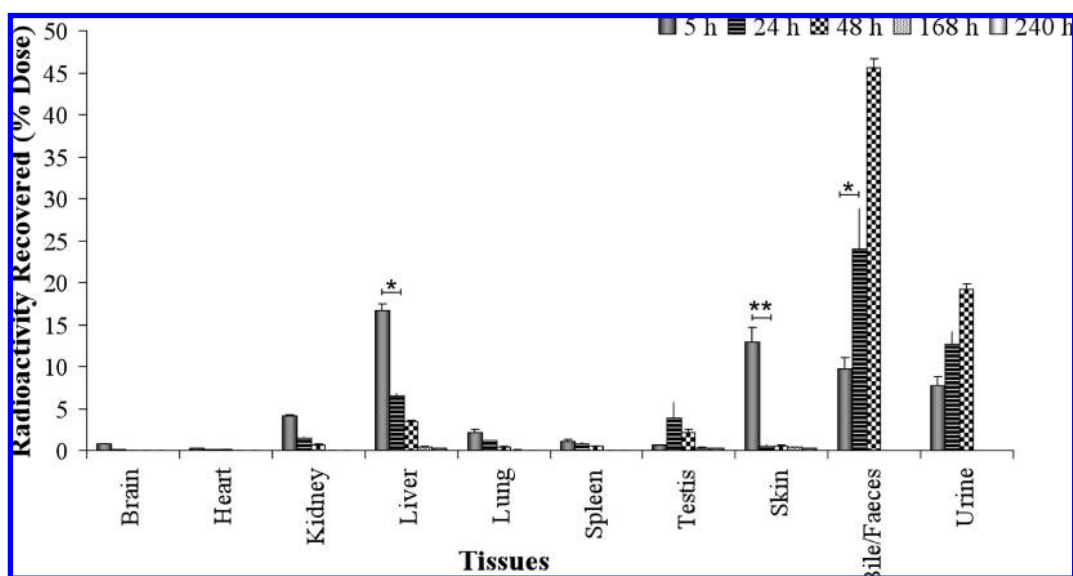

Figure 6. Percentage of radioactive dose recovered in tissues 5, 24, 48, 168, and 240 h after administration of [^{3}H]**2k** (54 μmol/kg, 20 μCi/rat) to male Wistar rats ($n = 4$). Results are expressed as mean percentage of dose $\pm$ SEM. Statistics were performed using a one-way ANOVA test for parametric data and Kruskal–Wallis test for nonparametric data: (*) $P < 0.05$; (**) $P < 0.01$; (***) $P < 0.001$.

Table 9. Summary of the Metabolites Produced in the Bile and Urine of Male Wistar Rats after Dosing with [^{3}H]**2k** (54 μmol/kg, 20 μCi)[a]

metabolite	retention time (min)	m/z	metabolite identity	metabolite proportion (% of radiolabeled metabolites, 0–5 h)	excreted in bile/urine
I–III[b]	3.60, 3.80, 6.26	ND[c]	ND[c]	2.43 $\pm$ 0.21, 0.47 $\pm$ 0.03, 3.57 $\pm$ 2.31	bile and urine
IV	8.36	469	ND[c]	62.5 $\pm$ 9.37	bile
V	12.36	358	**2k**	5.35 $\pm$ 2.22, 67.53 $\pm$ 9.22	bile and urine
VI	16.26	ND[c]	ND[c]	19.0 $\pm$ 3.49	bile
VII	10.91	388	carboxylic acid in side chain of **2k**	14.22 $\pm$ 2.21	urine
VIII	13.8	374	**2k**-*N*-oxide	3.55 $\pm$ 0.21	urine
IX	15.75	564	glucuronide of carboxylic acid side chain derivative	9.95 $\pm$ 3.11	urine

[a] Metabolites were characterised by LC–MS. [b] Metabolites **I–III** were minor metabolites. [c] ND = not determined.

metabolites was observed, as indicated by the lack of glutathione conjugate formation.

Pharmacokinetics

Given the higher potency of **2k** in the in vivo studies, this molecule was selected for comparative pharmacokinetic studies following iv and po administration to the mouse and rat. For the purposes of comparison we included two other lead 4-aminoquinolines **1d** and **1f** as comparators. Table 11 compares the blood clearance and oral bioavailability in the mouse and the rat. Blood clearance of comparator molecule **1d** was very high, exceeding the rate of blood flow to the liver in both species

Scheme 5. Structures of the Metabolites Identified in the Bile and Urine of Male Wistar Rats Dosed iv with [³H]**2k** (54 μmol/kg, 20 μCi)[a]
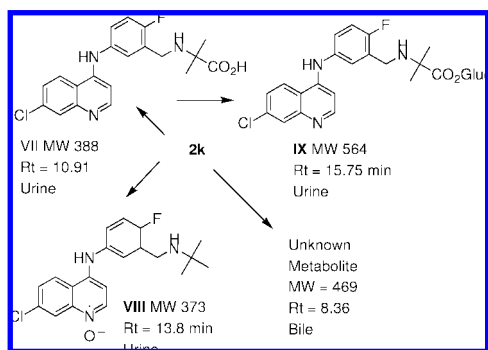
[a] Gluc = glucuronide.

Scheme 6. Structures of the Metabolites Identified in the Bile and Urine of Male Wistar Rats Dosed iv with [³H]**3k** (54 μmol/kg, 20 μCi)
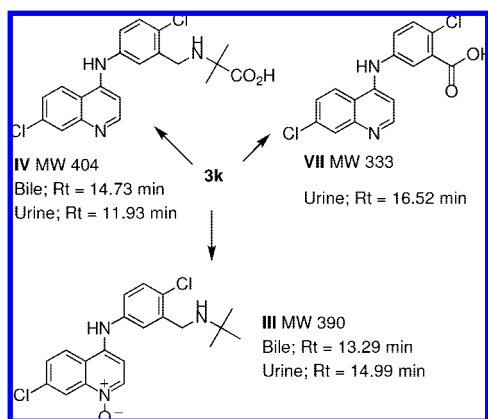
studied. Mean oral bioavailability of this molecule was less than 20%. Both **1f** and **2k** had substantially lower blood clearance compared to **1d**. The oral bioavailability of **2k** was 100% in the rat and 37% in the mouse in contrast to **1d** which had low clearance values of 21% and 17%, respectively.

In terms of the pharmacokinetics of **2k** in the mouse, exposure was comparable to chloroquine after administration of a single 10 mg/kg oral dose of drug with equivalent AUC over 24 h and similar elimination half-lives (~7 h in noninfected mice) (Figure 7). Whole blood concentrations were significantly higher in infected animals compared to noninfected animals (data not shown). This presumably represents selective accumulation into parasitized red cells as seen in in vitro studies. The poor exposure to amodiaquine in studies conducted in infected animals reflects its efficient first pass metabolism to desethyl amodiaquine in vivo.

Intrinsic Clearance. Intrinsic clearance of **2k** and related 4-aminoquinoline derivatives was compared in animal and human hepatocytes in vitro. The results are summarized in Table 12. As expected, amodiaquine had high intrinsic clearance in mouse, rat, dog, monkey, and human hepatocytes. Isoquine had high intrinsic clearance in mouse, rat, dog, and monkey hepatocytes but moderate intrinsic clearance in human hepatocytes. The major metabolite of amodiaquine, the result of N-dealkylation, had lower intrinsic clearance compared to the parent drug. Compared with amodiaquine and isoquine, **2k** had lower intrinsic clearance across all species.

Human P450 Inhibition. The potential for inhibition of the major human cytochrome P450 isozymes was compared for related 4-aminoquinoline derivatives, using sensitive screening assays employing purified recombinant enzymes and fluorescent probe substrates. The results of these studies are summarized in Table 13. Inhibition of 2D6-mediated 4-methylamino-7-methoxycoumarin O-dealkylation was observed for isoquine, amodiaquine, desethyl amodiaquine, and **2k**. For this isozyme, IC_{50} values ranged from 0.3 to 7 μM across this series.

In Vitro Cytotoxicity Studies in Rat Hepatocytes. Rat hepatocytes, isolated using a two-step collagen digestion method (Supporting Information), were incubated with amodiaquine, **2k**, or **3k** at concentrations of 0, 20, 50, 100, 200, and 500 μM (Figure 8). Results are expressed as the percentage of viable cells, measured microscopically, using a trypan blue exclusion test (as a percentage of the control). The results from this study show that the most profound difference in toxicity for rat hepatocytes was observed with **2k** (Figure 8). By replacement of the hydroxyl group of amodiaquine with fluorine and incorporation of a *tert*-butyl group into the amine side chain, the TD_{50} decreases from 78 to 385 μM, a 5-fold difference. **3k** also showed less toxicity than amodiaquine after incubation with rat hepatocytes, although to a lesser extent than **2k** (TD_{50} = 120 μM). The in vitro therapeutic indexes of **2k** and **3k** were observed to be very high at 29 167 and 11 881, respectively, showing that the amount of compound required to kill the parasite is much lower than that which causes toxicity to hepatocytes (Table 14).

Genotoxicity. The potential genotoxicity of **2k** and **3k** has been determined by the *Salmonella typhimurium* SOS/*umu* assay in two strains: TA1535/pSK1002 and NM2009.[38] This assay is based on the ability of DNA damaging agents to induce the expression of the *umu* operon. The *Salmonella* strains have a plasmid pSK1002 that carries a *umu*C-lacZ fused gene that produces a hybrid protein with β-galactosidase activity and whose expression is controlled by the *umu* regulatory region. Since many compounds do not exert their mutagenicity effect until they have been metabolized, the assay was also performed in the presence of rat liver S9-mix. Positive control agents (4-nitroquinoline 1-oxide and 2-aminoanthracene) were used to test the response of the tester strains. Both **2k** and **3k** were negative at the highest concentration tested (140 μM).[38]

Preliminary in Vivo Toxicity in Uninfected (Healthy) Mice. The final part of this study was to determine the no observed adverse effects level (NOAEL) of **2k** in the mouse after oral administration of either a single dose or four doses (single daily dose for 4 days according to the same administration schedule used in therapeutic efficacy studies). Chloroquine and amodiaquine were included as control compounds.

The dose framework for NOAEL definition was established from oral MNLD (maximal nonlethal dose) determinations shown in Table 15. The parameters evaluated for oral NOAEL included major apparent signs of toxicity after dosing, body weights evolution, biochemical analysis of serum (general, hepatic and renal toxicity biomarkers), and hematology evaluation. A summary of results can be found in Table 16.

The three 4-aminoquinoline derivatives appeared to have similar toxicities with NOAELs of 100 mg/kg for the four oral doses, with 300 mg/kg being the first dose with detected toxic effects. The four oral dose NOAELs for amodiaquine and chloroquine were 100 and 300 mg/kg, respectively; for **2k** the four oral dose NOAEL was 100 mg/kg.

Discussion

The necessity for a new 4-aminoquinoline antimalarial to supersede chloroquine and amodiaquine is apparent. The

Table 10. Summary of the Metabolites Produced in the Bile and Urine of Male Wistar Rats after Dosing with [^{3}H]**3k** (54 μmol/kg, 20 μCi)[a]

metabolite	retention time (min)	m/z	metabolite identity	metabolite proportion (% of radiolabeled metabolites, 0–5 h)	excreted in bile/urine
I,[b] **II**,[b] **V**, and **VI**	7.30, 8.02, 16.09, 18.09	ND[c]	ND[c]	1.08 ± 0.21, 1.63 ± 0.26, 12.48 ± 2.94, 19.53 ± 6.82	bile
III	13.29, 14.99	390	**3k**-N-oxide	4.52 ± 0.03, 34.43 ± 1.67	bile and urine
IV	14.73, 11.93	404	carboxylic acid side chain derivative of **3k**	60.76 ± 2.34 28.48 ± 3.33	bile and urine
VII	13.46	374	parent compound **3k**	55.70 ± 6.31	urine
VIII	16.52	333	benzoic acid derivative of **3k**	11.39 ± 2.99	urine

[a] Metabolites were characterised by LC−MS. [b] Metabolites **I** and **II** were minor metabolites. [c] ND = not determined.

Table 11. Blood Clearance and Oral Bioavailability of Desethylisoquine (**1f**), Isoquine (**1d**), and **2k** in Animals[a]

parameter	species	1f	1d	2k
blood clearance ((mL/min)/kg)	mouse	43.5	219	40.4
blood clearance ((mL/min)/kg)	rat	61.5 ± 21.6	89.2 ± 4.3	35 ± 4.2
oral F (%)	mouse	100	21	37
oral F (%)	rat	60 ± 26	17.0 ± 4.0	100

[a] For studies of the rat, data are expressed as mean ± SD (n = 3). For composite mouse studies variability of parameters has not been estimated.
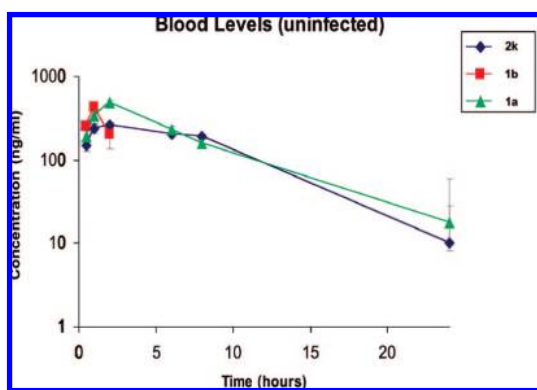
Figure 7. Concentration−time profile for **2k**, amodiaquine (**1b**), chloroquine (**1a**), in the uninfected mouse after a single oral dose of 10 mg/kg.

PfCRT-mediated resistance to chloroquine[11] and the toxicity of amodiaquine have prompted a re-examination of the pharmacology of new and existing 4-aminoquinoline antimalarials.[22] Piperaquine (**9**), a bisquinoline compound (Chart 2), is currently undergoing phase III trials in combination with dihydroartemisinin (DHA).[39,40] Piperaquine was introduced as a monotherapy for the treatment of malaria in the 1960s, and it was considered at least as effective as chloroquine against *P. falciparum* and *P. vivax* malaria and was considered to be better tolerated. Its use declined in the 1980s because of the emergence of piperaquine-resistant strains of *P. falciparum* and the availability of the artemisinin derivatives.[41] In the 1990s, a group of Chinese scientists rediscovered piperaquine and used it as one of the components of short-course artemisinin-based combination therapies to achieve a high cure rate without significant adverse effects. A number of clinical trials carried out by White et al. describe dihydroartemisinin (DHA)/piperaquine as a highly efficacious and well-tolerated combination therapy for the treatment of malaria.[40] Concerns with this combination lie in the fact that the calculated terminal half-life for piperaquine is around 16.5 days.[42] Compared to that of DHA (approximately 0.5 h),[43] the development of resistance could be a possibility due to prolonged exposure of piperaquine at subtherapeutic levels and the prior emergence of extensive parasites' resistant to monotherapy with this drug in China. Of

equal concern is that the long half-life of piperaquine may lead to toxicity through accumulation, as has been observed for chloroquine. Piperaquine does not, however, contain any obvious structural alert for metabolic activation.

Given the half-life issues with **9**, it is important to identify and design a drug from the 4-aminoquinoline class that has a half-life shorter than the half-lives of chloroquine and amodiaquine. As noted earlier, our approach to addressing the toxicity concerns with amodiaquine has involved two different strategies to modify the 4-aminophenol unit. The first approach involved the interchange of the hydroxyl group of amodiaquine with the amino side chain leading to the isoquine series of amodiaquine analogues. Following extensive antimalarial and preclinical evaluation *N-tert*-butylisoquine (**1e**) was selected from this group as a drug for clinical trials in humans and the phase 1 study was initiated in April 2008. On the basis of the concept of removing the 4-aminophenol "metabolic alert", a number of different groups have prepared novel amodiaquine derivatives. For example, Sergheraert and co-workers have synthesized a series of novel 4-aminoquinolines that retain the aromatic ring of amodiaquine but lack the 4′-hydroxyl group responsible for the transformation to the toxic quinoneimine in vivo (Chart 2, e.g., **10**).[44] The strategy of the Sergheraert group involved the incorporation of a basic side chain in both the 3′ and 4′ positions of the aromatic nucleus to prevent nucleophilic addition of proteins during metabolism. The results of this work revealed several compounds with high antimalarial activity, with no cross-resistance in vitro and low cytotoxicity in tests using a human lung cell line.[44]

More recently, similar structural modifications to tebuquine (3-((*tert*-butylamino)methyl)-4′-chloro-5-(7-chloroquinolin-4-ylamino)biphenyl-2-ol) have been reported. Lin described a series of isotebuquine analogues (**11**) with a hydroxy group meta rather than para to the amino group of the aniline moiety (Chart 2).[45] In vitro testing of these novel isotebuquine analogues against chloroquine-sensitive and chloroquine-resistant parasites showed them to exhibit activity similar to that of tebuquine.[45] However, during in vivo analysis the new isotebuquine analogues showed only marginal antimalarial activity, possibly due to poor solubility in vehicle and water.[45] Sparatore and co-workers also have designed isoquine and tebuquine analogues, and some of these compounds (for example, pyrrole derivative **12**) have good activity versus chloroquine resistant strains of *P. falciparum*.[46] Other 4-aminoquinolines under development include the chloroquine analogue N^1-(7-chloroquinolin-4-yl)-N^4,N^4-diethylbutane-1,4-diamine (AQ13)[47] and the organometallic analogue ferroquine (7-chloro-4-[(2-*N*,*N*-dimethylaminomethyl)ferrocenylmethylamino]quinoline),[48] both of which have entered clinical trials in man.

In this publication we have presented extensive metabolic and dispositional studies on candidates **2k** and **3k**, making direct comparisons to chloroquine, amodiaquine, and isoquine (**1d**). Each compound was synthesized via highly efficient and

Table 12. Comparison of the Intrinsic Clearance of Isoquine, Amodiaquine, Desethylamodiaquine, and **2k** in Animal and Human Hepatocytes

	intrinsic clearance ((mL/min)/g liver)				
compd	mouse	rat	dog	monkey	human
amodiaquine (**1b**)	>50	9.9 ± 5.3	12.0 ± 0.5	29 ± 1	9.8 ± 0.2
isoquine (**1d**)	41 ± 7	11 ± 4	23 ± 1	21 ± 1	3.3 ± 0.1
desethylamodiaquine	11 ± 2	1.9 ± 0.4	4.4 ± 0.3	1.6 ± 0.2	<0.5
2k	16 ± 1.2	3.6 ± 0.7	4.5 ± 1.0	12.3 ± 1.1	2.96 ± 0.3

Table 13. Comparative P450 Inhibition Potential of Isoquine, Amodiaquine, Desethylamodiaquine, and **2k**[a]

	inhibition potential IC_{50} (μM)						
compd	3A4 DEF	3A4 PPR	1A2	2D6	2C8	2C9	2C19
amodiaquine (**1b**)	28 ± 6	>100	15 ± 5	6.1 ± 0.5	2.7 ± 1.4	62 ± 9	≥85
isoquine (**1d**)	A[b]	>100	23 ± 8	7.0 ± 0.2	13 ± 2	75 ± 8	39 ± 11
desethyl amodiaquine	24 ± 3	>100	28 ± 11	6.4 ± 0.1	20 ± 4	58 ± 2	54 ± 11
2k	A[b]	>100	8.8 ± 1.9	0.3 ± 0.1	9.8 ± 3.9	52, >100	64, >100

[a] Mean and standard deviation of three independent IC_{50} (μM) determinations reported. [b] Activation observed.
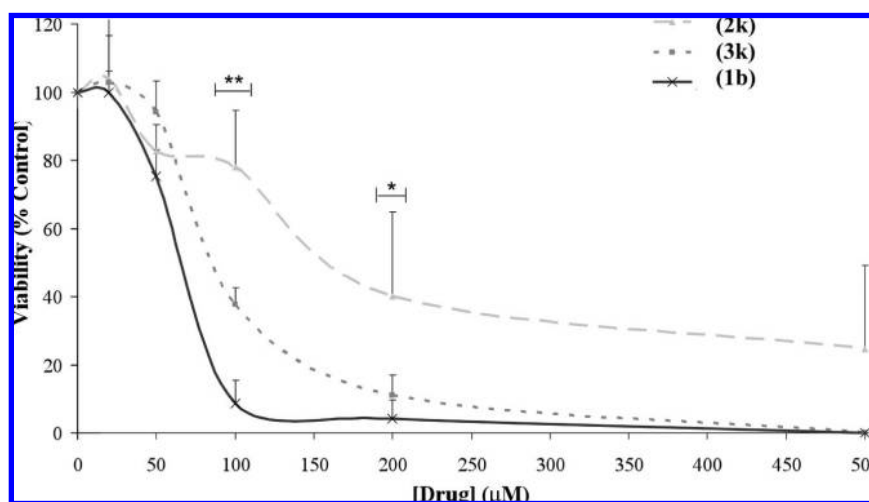
Figure 8. Viability of male Wistar rat hepatocytes incubated for 6 h with various concentrations of **2k** or **3k** and stained with trypan blue dye as an indicator for cell death. Results are expressed as mean percentage of dose ± SEM. Statistics were performed using a one-way ANOVA test for parametric data and Kruskal–Wallis test for nonparametric data: (*) $P < 0.05$; (**) $P < 0.01$; (***) $P < 0.001$.

Table 14. In Vitro Therapeutic Index of Amodiaquine, **2k**, and **3k** as a Measure of the Cytotoxicity in Male Wistar Rat Hepatocytes

compd	IC_{50} HB3 strain (nM)	Tox_{50} rat hepatocytes (μM)	in vitro therapeutic index
amodiaquine (**1b**)	8.5 ± 3.4	78 ± 2.3	9176
2k	14.6 ± 5.4	385 ± 25.6	26369
3k	8.1 ± 3.2	120 ± 14.5	14814

Table 15. Single Oral Dose Maximal Nonlethal Dose (MNLD)

compd	route	MNLD (mg/kg)
chloroquine (**1a**)	po	840
amodiaquine (**1b**)	po	>500
2k	po	610

inexpensive routes, allowing for in depth in vitro and in vivo pharmacological testing to be performed. More importantly, the chemistry should enable the delivery of 4-aminoquinolines with acceptable cost of goods based on the commercial costs of starting materials. It is clear from the studies that fluoro and chloro analogues of amodiquine have excellent in vitro antimalarial activity against a range of different strains of *Plasmodium falciparum* including chloroquine-resistant parasites such as TM6, K1, TM4, V1S, and J164.

In terms of mechanism of action we have definitively shown that both **2k** and **3k** have identical activity in the BHIA assay;[37] in terms of equilibrium binding **2k** had similar equilibrium binding constants to both chloroquine and amodiaquine, sug-

gesting a common mechanism of action. Table 17 contains measured pK_a values for amodiaquine, chloroquine, **2k**, and **3k**. On the basis of these data, we have calculated the ClogP and log D at medium pH (7.4). From these values and the drug pK_a values we have estimated the vacuolar accumulation ratio (VAR) and lipid accumulation ratio (LAR) of each drug, using the model of Warhurst et al.[49] and assuming a digestive vacuole pH of 5.2.[50] There is a good range of in vitro antimalarial activity (4-fold) among these compounds, but their interaction with hematin is very similar (Table 8). Since the differences in activity cannot be attributed to their hematin binding affinities, it is interesting to compare the VAR and LAR accumulation parameters to gain some insights into the antimalarial mode of action of these drugs (Table 17). Considering the very high predicted accumulation of diprotic weak bases in the acid vacuole water by a proton trapping mechanism, it is tempting to speculate that the important drug–heme interaction is taking place in the aqueous environment. If so, then we would expect the VAR to be well correlated with antimalarial activity. On the contrary, the drugs with the highest VAR (e.g., chloroquine) have the lowest antimalarial activity and vice versa. In fact, antimalarial activity appears to be well correlated with the LAR among this series of 4-aminoquinolines ($R^2 = 0.97$). These findings suggest that the interaction of hematin with uncharged drug species may be more important than previously suspected. These data should be considered in light of recent findings from

Table 16. NOAEL (No Observed Adverse Effect Levels)[a]

compd	NOAEL, 1 dose (mg/kg)	NOAEL, 4 doses (mg/kg)	toxicity observed above NOAELs
chloroquine (**1a**)	300	300	hepatic toxicity (ALP, ALT, AST, LAP), steatosis
amodiaquine (**1b**)	100	100	hepatic (LAP, CHOL, AST) and hematological (neutrophils) toxicity
2k	300	100	hepatic (ALT, AST, TBIL, TG), renal (BUN), and hematological (neutrophils) toxicity

[a] Single and four oral doses.

Chart 2. 4-Aminoquinoline Derivatives

4-Aminoquinoline derivatives
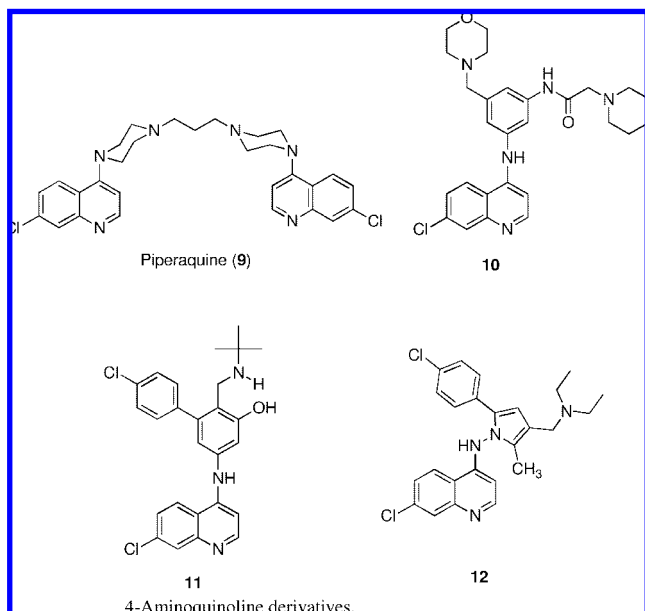
the Sullivan laboratory, that hemozoin microcrystals appear to be surrounded by neutral lipid "nanospheres" inside the digestive vacuole.[51,52]

Following the in vitro analysis of both sets of molecules, **2k** and **3k** were examined in the Peter's 4-day test.[28] The fluoro analogue **2k** was slightly less potent than amodiaquine and isoquine; chloro analogue **3k**, although more potent than amodiaquine in vitro, was significantly less potent in the mouse model with an ED$_{50}$ of 13 mg/kg.

The disposition studies reveal a similar pattern to other 4-aminoquinolines in the class, and metabolism studies confirm that both **2k** and **3k** do not produce aminophenol metabolites capable of undergoing oxidation to chemically reactive quinoneimines or other electrophilic metabolites. This demonstrates that halogenation of the arylamino ring system imparts metabolic stability for these compounds. Since **2k** outperformed **3k** in the

4-day test, **2k** was selected for further profiling. In comparison to isoquine (**1d**), **2k** had moderate to excellent oral bioavailability in the two animal studies performed. Overall, the exposure pharmacology of **2k** appears to be similar to chloroquine whereas total radioactivity distribution of this fluorinated analogue reflects that of amodiaquine. Fluoro analogue **2k** was shown to inhibit CYP 2D6 which was predicted since many drugs in this class have this potential.[54] Both **2k** and **3k** demonstrate excellent in vitro safety profiles with large therapeutic indices when antimalarial activity is compared to mammalian cytotoxicity. In preliminary screens we have demonstrated a lack of mutagenicity, and in vivo MNLD and NOEL were similar for **2k**, chloroquine, and amodiaquine.

In conclusion, fluoro analogue **2k** represents an excellent candidate for further studies with potent activity against chloroquine-resistant parasites, an excellent safety profile, and acceptable pharmacokinetic and exposure profiles. These results establish *N-tert*-butylfluoro amodiaquine (**2k**) as a suitable backup compound for clinical candidate *N-tert*-butylisoquine (**1e**).

Experimental Section

All reactions that employed moisture sensitive reagents were performed in dry solvent under an atmosphere of nitrogen in oven-dried glassware. All reagents were purchased from Sigma Aldrich or Alfa Aesar chemical companies and were used without purification. Thin layer chromatography (TLC) was carried out on Merck silica gel 60 F-254 plates, and UV inactive compounds were visualized using iodine or anisaldehyde solution. Flash column chromatography was performed on ICN Ecochrom 60 (32−63 mesh) silica gel eluting with various solvent mixtures and using an air line to apply pressure. NMR spectra were recorded on a Brucker AMX 400 (^{1}H, 400 MHz; ^{13}C, 100 MHz) spectrometer. Chemical shifts are described on parts per million (δ) downfield from an internal standard of trimethylsilane. Microanalyses were performed in the University of Liverpool Microanalysis Laboratory. Mass spectra were recorded on a VG analytical 7070E machine and Fisons TRIO spectrometers using electron ionization (EI) and chemical ionization (CI).

Chemistry. General Procedure 1. To a solution of fluoroaldehyde (250 mg) in dry CH$_2$Cl$_2$ (10 mL) and dry DMF (0.25 mL) was added the appropriate amine (5 equiv). The mixture was

Table 17. Measured pK_a Values, ClogP, log *D*, Vacuolar Accumulation Ratio (VAR), and Lipid Accumulation Ratio (LAR) for Selected 4-Aminoquinolines[a]

drug (IC$_{50}$ HB3 strain)	equation	measured pK_a	ClogP	log *D* (7.4)	VAR (pHvac = 5.2)	LAR
amodiaquine (5.5 nM)	X$^-$ + H$^+$ ⇌ XH	11.73 ± 0.31	4.24	3.08	10756.8	908.4
	XH + H$^+$ ⇌ XH$_2^+$	8.40 ± 0.12	4.24	3.08	10756.8	908.4
	XH$_2^+$ + H$^+$ ⇌ XH$_3^{2+}$	7.31 ± 0.18	4.24	3.08	10756.8	908.4
chloroquine (20.2 nM)	B + H$^+$ ⇌ BH$^+$	10.31 ± 0.46	4.79	0.06	21834.0	9.97
	BH$^+$ + H$^+$ ⇌ BH$_2^{2+}$	8.22 ± 0.27	4.79	0.06	21834.0	9.97
2k (14.6 nM)	B + H$^+$ ⇌ BH$^+$	9.45 ± 0.26	4.87	2.40	12151.7	340.1
	BH$^+$ + H$^+$ ⇌ BH$_2^{2+}$	7.37 ± 0.39	4.87	2.40	12151.7	340.1
3k (8.1 nM)	B + H$^+$ ⇌ BH$^+$	9.33 ± 0.42	5.32	3.00	9474.0	1520.6
	BH$^+$ + H$^+$ ⇌ BH$_2^{2+}$	7.18 ± 0.38	5.32	3.00	9474.0	1520.6

[a] The sample pK_a values were determined using the fast-DPAS ((D-PAS = dip probe absorption spectroscopy) method. All samples were titrated at a concentration of ~50 μM between pH 2 and pH 12. All pK_a values were obtained by extrapolating the data to aqueous conditions by the Yasuda−Shedlovsky method (see http://www.sirius analytical.com). From measured pK_a values, the vacuolar accumulation ratio (VAR) and lipid accumulation ratio (LAR) of each drug were determined using the model of Warhurst et al.[49] and assuming a digestive vacuole pH of 5.2.[50] ClogP values were calculated using the AlogPS 2.1 program.[53]

allowed to stir at room temperature for 2 h. After this time, NaHB(OAc)$_3$ (0.50 g, 3 equiv) was added to the solution and the mixture was stirred overnight at room temperature. The solvent was removed in vacuo and the residue was purified via column chromatography (10% MeOH in CH$_2$Cl$_2$) to give the desired product.

N-(3-((Diethylamino)methyl-4-fluorophenyl)-7-chloroquinolin-4-amine (2d). The sample was prepared according to general procedure 1 using diethylamine to give **2d** as a yellow solid: 0.14 g, 24%; mp = 130−133 °C; ^{1}H NMR (CDCl$_3$, 400 MHz) δ 8.50 (1H, d, J = 5.32 Hz, Ar−H), 8.02 (1H, d, J = 2.04 Hz, Ar−H), 7.85 (1H, d, J = 8.96 Hz, Ar−H), 7.45 (2H, m, Ar−H), 7.17 (1H, m, Ar−H), 7.10 (1H, dd, J = 8.96, 2.04 Hz, Ar−H), 6.80 (1H, d, J = 5.32 Hz, Ar−H), 6.61 (1H, s, NH), 3.65 (2H, s, CH$_2$N), 2.60 (4H, q, J = 7.12 Hz, 2 × CH$_2$), 1.06 (6H, t, J = 7.10 Hz, 2 × CH$_3$); ^{13}C NMR (CDCl$_3$, 100 MHz) δ 160.2, 157.8, 152.3, 150.0, 148.8, 135.5, 129.3, 128.9, 126.7, 126.4, 123.9, 121.6, 118.2, 116.5, 102.3, 50.2, 47.5, 12.2; MS (CI) m/z 358 [M + H]$^+$ (100), 360 (32), 253 (44), 74 (72); HRMS m/z 358.148 19 (C$_{20}$H$_{22}$^{35}ClFN$_3$ requires 358.148 62). Anal. (C, H, N).

7-Chloro-N-(4-fluoro-3-((pyrrolidin-1-yl)methyl)phenyl)quinolin-4-amine (2e). The sample was prepared according to general procedure 1 to give **12e** as a yellow solid: 0.06 g, 20%; mp = 156−158 °C; ^{1}H NMR (CDCl$_3$, 400 MHz) δ 8.55 (1H, d, J = 9.10 Hz, Ar−H), 8.45 (1H, d, J = 6.54 Hz, Ar−H), 7.95 (1H, d, J = 2.09 Hz, Ar−H), 7.82 (1H, dd, J = 6.33, 2.68 Hz Ar−H), 7.70 (1H, dd, J = 9.10, 2.09 Hz Ar−H), 7.62 (1H, m, Ar−H), 7.42 (1H, t, J = 9.18 Hz, Ar−H), 7.02 (1H, d, J = 6.54 Hz, Ar−H), 4.90 (1H, s, NH), 3.70 (2H, s, CH$_2$N), 3.45 (4H, m, 2 × NCH$_2$), 2.10 (4H, m, 2 × CH$_2$); ^{13}C NMR (CDCl$_3$, 100 MHz) δ 162.6, 160.1, 155.4, 147.9, 144.3, 140.4, 136.5, 130.9, 130.6, 129.0, 126.3, 123.5, 121.6, 119.3, 102.9, 55.6, 52.4, 24.4; MS (CI) m/z 356 ([M + H]$^+$, 100), 358 (32), 253 (54), 70 (72); HRMS m/z 356.132 77 (C$_{20}$H$_{20}$^{35}ClFN$_3$ requires 356.132 97). Anal. (C, H, N).

7-Chloro-N-(4-fluoro-3-((piperidin-1-yl)methyl)phenyl)quinolin-4-amine (2f). The sample was prepared according to general procedure 1 using piperidine to give **2f** as a yellow solid: 0.19 g, 31%; mp = 195−201 °C; ^{1}H NMR (CDCl$_3$, 400 MHz) δ 8.54 (1H, d, J = 5.25 Hz, Ar−H), 8.03 (1H, d, J = 2.02 Hz, Ar−H), 7.85 (1H, d, J = 8.99 Hz, Ar−H), 7.45 (1H, dd, J = 8.99, 2.02 Hz, Ar−H), 7.35 (1H, dd, J = 6.53, 2.95 Hz, Ar−H), 7.20 (1H, m, Ar−H), 7.12 (1H, t, J = 8.81 Hz, Ar−H), 6.80 (1H, d, J = 5.25 Hz, Ar−H), 6.50 (1H, bs, NH), 3.56 (2H, s, CH$_2$N), 2.51 (4H, m, 2 × CH$_2$N), 1.52−1.47 (6H, m, 3 × CH$_2$); ^{13}C NMR (CDCl$_3$, 100 MHz) δ 157.7, 1521, 150.0, 148.6, 135.6, 129.6, 128.9, 126.8, 126.5, 123.5, 121.3, 118.1, 116.5, 102.4, 100.1, 55.8, 46.4, 27.5, 25.4; MS (CI) m/z 370 ([M + H]$^+$, 100), 372 (30), 253 (42), 86 (85); HRMS m/z 370.147 68 (C$_{21}$H$_{22}$^{35}ClFN$_3$ requires 370.148 62). Anal. (C, H, N).

7-Chloro-N-(4-fluoro-3-((4-methylpiperazin-1-yl)methyl)phenyl)quinolin-4-amine (2g). The sample was prepared according to general procedure 1 using piperidine to give **2f** as a yellow solid: 0.20 g, 31%; mp = 165−169 °C; ^{1}H NMR (400 MHz, CDCl$_3$) δ 8.54 (1H, d, J = 5.33 Hz, Ar−H); 8.01 (1H, d, J = 2.10 Hz, Ar−H), 7.90 (1H, d, J = 8.96 Hz, Ar−H), 7.41 (1H, dd, J = 2.10 Hz, 8.96 Hz, Ar−H), 7.34 (1H, dd, J = 2.72 Hz, 6.22 Hz, Ar−H), 7.18 (1H, m, Ar−H), 7.08 (1H, t, J = 8.95 Hz, Ar−H), 6.80 (1H, d, J = 5.33 Hz, Ar−H), 3.60 (2H, s, CH$_2$N), 2.60 (4H, s, 2 × CH$_2$N), 2.54 (4H, s, 2 × CH$_2$N), 2.25 (3H, s, CH$_3$−N); ^{13}C NMR (400 MHz, CDCl$_3$) δ 160.3, 157.9, 152.2, 150.0, 148.8, 135.8, 129.2, 126.9, 126.4, 124.4, 121.8, 118.2, 116.9, 116.7, 102.3, 55.4, 55.3, 53.1, 46.0; MS (CI) m/z 385 ([M + H]$^+$, 100), 387 (27), 389 (2); HRMS m/z 385.158 06 (C$_{21}$H$_{22}$^{35}ClFN$_4$ requires 385.159 52). Anal. (C, H, N).

N-(3-((Dipropylamino)methyl)-4-fluorophenyl)-7-chloroquinolin-4-amine (2h). The sample was prepared according to general procedure 1 using dipropylamine to give **2h** as a yellow solid: 0.17 g, 27%; mp = 130−132 °C; ^{1}H NMR (400 MHz, CDCl$_3$) δ 8.45 (1H, d, J = 5.32 Hz, Ar−H), 8.01 (1H, d, J = 1.94 Hz, Ar−H), 7.86 (1H, d, J = 8.92 Hz, Ar−H), 7.85 (1H, dd, J = 8.92, 1.94 Hz, Ar−H), 7.44 (1H, m, Ar−H), 7.15−7.04 (2H, m, Ar−H), 6.79

(1H, d, J = 5.32 Hz, Ar−H), 6.65 (1H, s, NH), 3.60 (2H, s, CH$_2$N), 2.39 (4H, m, 2 × NCH$_2$CH$_2$), 1.49 (4H, m, 2 × CH$_2$CH$_2$-CH$_3$), 0.83 (6H, t, J = 7.04 Hz, 2 × CH$_3$-CH$_2$); ^{13}C NMR (100 MHz, CDCl$_3$) δ 160.2, 152.4, 152.3, 150.1, 148.7, 135.7, 129.5, 126.7, 126.6, 123.9, 123.8, 121.5, 116.7, 116.5, 102.3, 62.8, 56.6, 51.3, 20.7, 12.3; MS (CI) m/z 386 ([M + H]$^+$, 100), 388 (30), 390 (1), 352 (100); HRMS m/z 386.179 55 (C$_{22}$H$_{26}$^{35}ClFN$_3$ requires 386.179 93). Anal. (C, H, N).

N-(3-((Dibutylamino)methyl)-4-fluorophenyl)-7-chloroquinolin-4-amine (2i). The sample was prepared according to general procedure 1 using dibutylamine to give **2i** as a yellow solid: 0.29 g, 42%; mp = 120−128 °C; ^{1}H NMR (CDCl$_3$, 400 MHz) δ 8.51 (1H, d, J = 5.49 Hz, Ar−H), 8.02 (1H, d, J = 2.19 Hz, Ar−H), 7.85 (1H, d, J = 9.07 Hz, Ar−H), 7.43 (2H, m, Ar−H), 7.15 (2H, m, Ar−H), 6.80 (1H, d, J = 5.49 Hz, Ar−H), 6.60 (1H, s, NH), 3.67 (2H, s, CH$_2$N), 2.50 (4H, t, J = 6.87 Hz, 2 × NCH$_2$), 1.20−1.55 (8H, m, 2 × CH$_2$CH$_2$), 0.89 (6H, t, J = 6.88 Hz, 2 × CH$_3$); ^{13}C NMR (CDCl$_3$, 100 MHz) δ 160.1, 157.7, 152.1, 150.1, 148.9, 135.7, 129.1, 128.9, 126.7, 126.4, 123.6, 121.6, 118.1, 116.5, 102.2, 53.7, 53.5, 32.2, 20.0, 13.7; MS (EI) m/z 414 [M + H]$^+$ (100), 416 (23); HRMS m/z 414.2097 (C$_{24}$H$_{30}$^{35}ClFN$_3$ requires 414.2112). Anal. (C, H, N).

7-Chloro-N-(4-fluoro-3-(morpholinomethyl)phenyl)quinolin-4-amine (2j). The sample was prepared according to general procedure 1 using dibutylamine to give **2j** as a yellow solid: 0.14 g, 23%; mp = 225−230 °C; ^{1}H NMR (CDCl$_3$, 400 MHz) δ 8.53 (1H, d, J = 5.26 Hz, Ar−H), 8.04 (1H, d, J = 2.06 Hz, Ar−H), 7.85 (1H, d, J = 8.94 Hz, Ar−H), 7.45 (1H, dd, J = 8.94, 2.06 Hz, Ar−H), 7.35 (1H, dd, J = 6.16, 2.57 Hz, Ar−H), 7.19 (1H, m, Ar−H), 7.11 (1H, t, J = 8.97 Hz, Ar−H), 6.80 (1H, d, J = 5.26 Hz, Ar−H), 6.60 (1H, bs, NH), 3.71 (4H, t, J = 4.48 Hz, 2 × CH$_2$O), 3.65 (2H, s, CH$_2$N), 2.55 (4H, t, J = 4.38 Hz, 2 × CH$_2$N); ^{13}C NMR (CDCl$_3$, 100 MHz) δ 157.8, 152.3, 150.1, 148.8, 135.8, 129.6, 128.9, 126.9, 126.6, 124.5, 121.4, 118.2, 116.5, 102.4, 100.0, 67.4, 55.8, 53.9; MS (CI) m/z 372 ([M + H]$^+$, 100), 374 (30), 253 (32), 88 (92); HRMS m/z 372.127 47 (C$_{20}$H$_{20}$^{35}ClFN$_3$O requires 372.127 87). Anal. (C, H, N).

[3-(*tert*-Butylaminomethyl)-4-fluorophenyl](7-chloro-quinolin-4-yl)amine (2k). The sample was prepared according to the method in Supporting Information from **4e** (by method in Scheme 3) to give **2k** as a pale-yellow solid: 0.37 g, 29%; ^{1}H (CDCl$_3$, 400 MHz) δ 8.52 (1H, d, J = 5.32 Hz, Ar−H), 8.02 (1H, d, J = 2.10 Hz, Ar−H), 7.83 (1H, d, J = 8.92 Hz, Ar−H), 7.43 (1H, dd, J = 2.10 Hz, 8.92 Hz, Ar−H), 7.35 (1H, dd, J = 2.68 Hz, 6.48 Hz, Ar−H), 7.18−7.13 (1H, m, Ar−H), 7.07 (1H, t, J = 8.92 Hz), 6.76 (1H, d, J = 5.32, Ar−H), 6.63 (1H, bs, NH), 3.80 (2H, s, CH$_2$), 1.18 (9H, s, (CH$_3$)$_3$); ^{13}C (100 Mz, CDCl$_3$) δ 160.0, 157.6, 152.4, 150.1, 148.6, 135.7, 129.5, 126.2, 126.2, 124.0, 121.4, 118.2, 116.8, 116.6, 102.4, 51.3, 40.8, 29.5; MS (CI) m/z 358 ([M + H]$^+$, 94), HRMS m/z 358.1488 (C$_{20}$H$_{22}$^{35}ClFN$_3$ requires 358.1486). Anal. (C, H, N).

General Procedure 2. HCl (5 drops) was added to a solution of the appropriate amine (0.52 mmol) and 4,7-dichloroquinoline (1 equiv) in EtOH (20 mL). The mixture was stirred at reflux for 24 h. The reaction mixture was concentrated, and 1 M NaOH was added to the residue. The aqueous mixture was washed with CH$_2$Cl$_2$ (×3). The organic layers were combined, dried over MgSO$_4$, filtered, and concentrated to give the crude product. Purification by column chromatography (silica gel, 10% MeOH in CH$_2$Cl$_2$) gave the desired product.

(7-Chloroquinolin-4-yl)(4-fluoro-3-imidazol-1-ylmethylphenyl)-amine (2l). General procedure 2 provided **2l** as an off-white solid: 0.91 g, 46%; ^{1}H (400 MHz, MeOD) δ 8.37 (1H, d, J = 5.56 Hz, Ar−H), 8.23 (1H, d, J = 9.03 Hz, Ar−H), 7.86 (1H, d, J = 2.28 Hz, Ar−H), 7.78 (1H, s, Ar−H), 7.49 (1H, dd, J = 2.09 Hz, 9.11 Hz, Ar−H), 7.37 (1H, m, Ar−H), 7.24 (2H, m, Ar−H), 7.17 (1H, s, Ar−H), 7.02 (1H, s, Ar−H), 6.78 (1H, d, J = 5.56 Hz, Ar−H), 4.82 (2H, s, CH$_2$); ^{13}C (100 MHz, MeOD) δ 160.7, 158.2, 152.7, 151.7, 150.4, 139.2, 138.3, 137.4, 130.0, 128.2, 127.4, 127.1, 125.0, 121.3, 119.8, 118.4, 118.1, 102.9, 45.8; MS (CI) m/z 353 ([M + H]$^+$, 100), 355 (32), 357 (1), 319 (34); HRMS m/z 353.095 93 (C$_{19}$H$_{15}$ClFN$_4$ requires 353.096 92). Anal. (C, H, N).

Compounds **3d−m** were prepared according to the general procedure 3 in Supporting Information.

***N*-(3-((Diethylamino)methyl)-4-chlorophenyl)-7-chloroquinolin-4-amine (3d).** Yellow solid; 0.22 g, 74%; ^{1}H NMR (CDCl$_3$, 400 MHz) δ 8.55 (1H, d, J = 5.28 Hz, Ar−H), 8.05 (1H, d, J = 2.09 Hz, Ar−H), 7.84 (1H, d, J = 8.96 Hz, Ar−H), 7.54 (1H, d, J = 2.71 Hz, Ar−H), 7.45 (1H, dd, J = 8.96, 2.09 Hz, Ar−H), 7.36 (1H, d, J = 8.46 Hz, Ar−H), 7.12 (1H, dd, J = 8.46, 2.77 Hz, Ar−H), 6.92 (1H, d, J = 5.28 Hz, Ar−H), 6.61 (1H, s, NH), 3.68 (2H, s, CH$_2$N), 2.60 (4H, q, J = 7.14 Hz, 2 × CH$_2$), 1.06 (6H, t, J = 7.10 Hz, 2 × CH$_3$); ^{13}C NMR (CDCl$_3$, 100 MHz) δ 152.3, 150.0, 147.9, 140.2, 138.9, 135.8, 130.6, 129.57, 129.21, 126.61, 124.6, 122.0, 121.5, 118.5, 103.0, 54.8, 47.8, 12.4; MS (CI) m/z 374 [M + H]$^+$ (100), 376 (73), 340 (28), 72 (24); HRMS m/z 374.118 83 (C$_{20}$H$_{22}$^{35}Cl$_2$N$_3$ requires 374.119 08) Anal. (C, H, N).

(4-Chloro-3-pyrrolidin-1-ylmethyl-phenyl)(7-chloroquinolin-4-yl)amine (3e). Yellow solid; 0.18 g, 61%; ^{1}H NMR (400 MHz, MeOD) δ 8.41 (1H, d, J = 5.52 Hz, Ar−H), 8.27 (1H, d, J = 8.99 Hz, Ar−H), 7.87 (1H, d, J = 2.04 Hz, Ar−H), 7.59 (1H, d, J = 2.67 Hz, Ar−H), 7.52−7.41 (2H, m, Ar−H), 7.28 (1H, dd, J = 2.04, 8.99 Hz, Ar−H), 6.97 (1H, d, J = 5.52 Hz, Ar−H), 3.81 (2H, s, CH$_2$), 2.66 (4H, s, CH$_2$−N-CH$_2$), 1.83 (4H, s, CH$_2$CH$_2$); ^{13}C NMR (100 MHz, MeOD) δ 152.9, 151.1, 150.7, 140.7, 139.0, 137.3, 131.9, 131.0, 128.3, 127.3, 126.9, 125.1, 124.7, 120.1, 103.5, 58.1, 55.5, 55.2, 24.8, 24.7; MS (CI) m/z 272 ([M + H]$^+$, 41), 269 (60); HRMS m/z 372.102 59 (C$_{20}$H$_{20}$Cl$_2$N$_3$ requires 372.103 42). Anal. (C, H, N).

7-Chloro-*N*-(4-chloro-3-((piperidin-1-yl)methyl)phenyl)quinolin-4-amine (3f). Yellow solid; 0.30 g, 92%; ^{1}H NMR (400 MHz, CDCl$_3$) δ 8.55 (1H, d, J = 5.25 Hz, Ar−H), 7.90 (1H, d, J = 2.06 Hz, Ar−H), 7.49 (1H, d, J = 2.57 Hz, Ar−H), 7.40 (1H, dd, J = 2.06, 8.90 Hz, Ar−H), 7.34 (1H, d, J = 8.90 Hz, Ar−H), 7.14 (1H, d, J = 2.7 Hz, Ar−H), 7.12 (1H, d, J = 2.7 Hz, Ar−H), 6.90 (1H, d, J = 5.25 Hz, Ar−H), 6.80 (1H, s, NH), 3.56 (2H, s, CH$_2$N), 2.46 (4H, t, J = 4.45 Hz, 2 × CH$_2$), 1.56 (4H, m, 2 × CH$_2$), 1.25 (2H, t, J = 7.15 Hz, CH$_2$); ^{13}C NMR (100 MHz, CDCl$_3$) δ 152.3, 150.2, 147.8, 138.7, 138.7, 135.8, 130.7, 130.0, 129.4, 126.6, 124.6, 122.2, 121.7, 118.6, 103.1, 60.1, 55.1, 53.8, 26.4, 24.6, 21.3; MS (CI) m/z 386 ([M + H]$^+$, 100), 388 (54); HRMS m/z 386.1191 (C$_{21}$H$_{22}$^{35}Cl$_2$N$_3$ requires 386.1167). Anal. (C, H, N).

7-Chloro-*N*-(4-chloro-3-((4-methylpiperazin-1-yl)methyl)phenyl)quinolin-4-amine (3g). Yellow solid; 0.28 g, 89%; ^{1}H NMR (400 MHz, CDCl$_3$) δ 8.54 (1H, d, J = 5.25 Hz, Ar−H), 8.01(1H, d, J = 2.10 Hz, Ar−H), 7.91 (1H, d, J = 9.06 Hz, Ar−H), 7.43 (1H, dd, J = 2.10, 9.06 Hz, Ar−H), 7.40 (1H, d, J = 2.07 Hz, Ar−H), 7.36 (1H, d, J = 8.42 Hz, Ar−H), 7.12 (1H, dd, J = 5.72, 8.42 Hz, Ar−H), 6.90 (1H, d, J = 5.25 Hz, Ar−H), 6.59 (1H, s, NH), 3.62 (2H, s, CH$_2$), 2.56 (4H, s, 2 × CH$_2$N), 2.43 (4H, s, 2 × CH$_2$N), 2.26 (3H, s, CH$_3$); ^{13}C NMR (100 MHz, CDCl$_3$) δ 151.8, 149.7, 147.6, 138.4, 137.8, 135.4, 130.4, 129.7, 128.9, 126.2, 124.4, 122.1, 121.5, 118.3, 102.7, 59.0, 55.2, 55.1, 53.2, 53.5, 46.0; MS (ES−) m/z 399 ([M − H]$^-$, 100), 401 (50), 403 (5); HRMS m/z 399.1154 (C$_{21}$H$_{21}$^{35}Cl$_2$N$_4$ requires 399.1143), 401.1118 (C$_{21}$H$_{21}$^{35}Cl^{37}ClN$_4$ requires 401.1114). Anal. (C, H, N).

***N*-(3-((Dipropylamino)methyl)-4-chlorophenyl)-7-chloroquinolin-4-amine (3h).** Yellow solid; 0.27 g, 85%; ^{1}H NMR (400 MHz, CDCl$_3$) δ 8.45 (1H, d, J = 5.32 Hz, Ar−H), 8.04 (1H, d, J = 2.08 Hz, Ar−H), 7.86 (1H, d, J = 8.92 Hz, Ar−H), 7.57 (1H, d, J = 2.63 Hz, Ar−H), 7.47 (1H, dd, J = 2.08, 8.92 Hz, Ar−H), 7.35 (1H, d, J = 8.36 Hz, Ar−H), 7.09 (1H, dd, J = 2.84, 8.36 Hz, Ar−H), 6.94 (1H, d, J = 5.32 Hz, Ar−H), 6.56 (1H, s, NH), 3.69 (2H, s, CH$_2$N), 2.46 (4H, t, J = 1.59 Hz, 2 × CH$_2$), 1.46 (4H, m, 2 × CH$_2$), 0.84 (6H, t, J = 7.31 Hz, 2 × CH$_3$); ^{13}C NMR (100 MHz, CDCl$_3$) δ 151.2, 149.1, 148.7, 139.7, 138.6, 136.2, 130.6, 129.9, 128.4, 128.2, 125.6, 124.9, 122.5, 122.4, 118.4, 102.7, 56.7, 55.8, 50.1, 20.5, 12.2; MS (ES−) m/z 400 ([M − H]$^-$, 100), 402 (45), 404 (3); HRMS m/z 400.1358 (C$_{22}$H$_{24}$Cl$_2$N$_3$ requires 400.1347). Anal. (C$_{22}$H$_{25}$Cl$_2$N$_3$) C, H, N.

(4-Chloro-3-dibutylaminomethylphenyl)(7-chloroquinolin-4-yl)amine (3i). Yellow solid; 0.08 g, 24%; ^{1}H (400 MHz, MeOD) δ 8.56 (1H, d, J = 5.27 Hz, Ar−H), 8.05 (1H, d, J = 2.11 Hz, Ar−H),

7.86 (1H, d, J = 8.98 Hz, Ar−H), 7.56 (1H, d, J = 2.43 Hz, Ar−H), 7.47 (1H, dd, J = 2.11, 8.98 Hz, Ar−H), 7.36 (1H, d, J = 8.46 Hz, Ar−H), 7.09 (1H, dd, J = 2.65, 8.53 Hz, Ar−H), 6.92 (1H, d, J = 5.27 Hz, Ar−H), 6.55 (1H, bs, NH), 3.69 (2H, s, CH$_2$), 2.48 (4H, t, J = 7.92 Hz, 2 × NCH$_2$), 1.45 (4H, m, CH$_2$CH$_2$NCH$_2$CH$_2$), 1.29 (4H, m, 2 × CH$_2$CH$_3$), 0.87 (6H, t, J = 7.32, 2 × CH$_2$CH$_3$); ^{13}C NMR (100 MHz, MeOD) δ 150.4, 148.9, 146.5, 138.7, 136.9, 136.6, 130.6, 126.6, 125.9, 125.7, 123.8, 123.3, 118.1, 101.8, 54.9, 53.4, 50.4, 32.8, 32.5, 22.6, 20.8, 20.5, 14.4, 14.2; MS (ES+) m/z 430 ([M + H]$^+$, 100); HRMS m/z 430.1804 (C$_{24}$H$_{30}$^{35}Cl$_2$N$_3$ requires 430.1817). Anal. (C, H, N).

7-Chloro-*N*-(4-chloro-3-((4-ethylpiperazin-1-yl)methyl)phenyl)quinolin-4-amine (3j). Yellow solid; 0.207 g, 63%; ^{1}H NMR (400 MHz, CDCl$_3$) δ 8.56 (1H, d, J = 5.32 Hz, Ar−H), 8.04 (1H, d, J = 2.08 Hz, Ar−H), 7.87 (1H, d, J = 8.92 Hz, Ar−H), 7.46 (1H, dd, J = 2.08, 8.92 Hz, Ar−H), 7.44 (1H, d, J = 2.64 Hz, Ar−H), 7.37 (1H, d, J = 8.52 Hz, Ar−H), 7.14 (1H, dd, J = 2.64 Hz, 8.52 Hz, Ar−H), 6.92 (1H, d, J = 5.32 Hz, Ar−H), 6.70 (1H, s, NH), 3.61 (2H, s, CH$_2$N), 2.47 (4H, bs, 2(−NCH$_2$−)), 2.57 (4H, bs, 2(−NCH$_2$−)), 2.40 (2H, q, J = 7.28 Hz, CH$_2$CH$_3$), 1.07 (3H, t, J = 7.20 Hz, CH$_3$CH$_2$); ^{13}C NMR (100 MHz, CDCl$_3$) δ 152.3, 150.2, 147.7, 138.7, 138.2, 135.8, 130.8, 130.1, 129.5, 126.6, 124.6, 122.4, 121.6, 118.6, 103.2, 59.4, 53.8, 53.5, 53.2, 52.7, 42.3, 12.1; MS (ES−) m/z 413 ([M − H]$^-$, 100), 415 (48), 417 (6); HRMS m/z 413.1297 (C$_{22}$H$_{23}$^{35}Cl$_2$N$_4$ requires 413.1300). Anal. (C, H, N).

[3-(*tert*-Butylaminomethyl)-4-chlorophenyl](7-chloroquinolin-4-yl)amine (3k). Yellow solid; (0.25 g, 59%); ^{1}H NMR (400 MHz, MeOD) δ 8.47 (1H, d, J = 5.72 Hz, Ar−H), 8.32 (1H, d, J = 8.92 Hz, Ar−H), 7.90 (1H, d, J = 2.12 Hz, Ar−H), 7.65 (1H, d, J = 2.64 Hz, Ar−H), 7.53 (2H, m, Ar−H), 7.39 (1H, dd, J = 2.64 Hz, 8.52 Hz, Ar−H), 7.08 (2H, d, J = 5.72 Hz, Ar−H), 4.81 (1H, bs, NH), 3.79 (2H, s, CH$_2$N), 1.21 (9H, s, (CH$_3$)$_3$); ^{13}C NMR (100 MHz, MeOD) δ 152.9, 150.9, 150.7, 140.9, 140.6, 137.2, 131.8, 130.6, 128.4, 127.3, 126.8, 125.0, 124.7, 120.1, 103.6, 52.7, 45.9, 29.3; MS (ES+) m/z 374 ([M + H]$^+$, 100), 376 (38), 378 (2); HRMS m/z 374.1187 (C$_{20}$H$_{22}$^{35}Cl$_2$N$_3$ requires 374.1191). Anal. (C, H, N).

7-Chloro-*N*-(4-chloro-3-((4-(pyridin-2-yl)piperazin-1-yl)methyl)phenyl)quinolin-4-amine (3l). Yellow solid: 0.36 g, 98%; ^{1}H NMR (400 MHz, CDCl$_3$) δ 8.57 (1H, d, J = 5.32 Hz, Ar−H), 8.17 (1H, m, −HC=N−), 8.04 (1H, d, J = 2.12 Hz, Ar−H), 7.87 (1H, d, J = 8.92 Hz, Ar−H), 7.51 (1H, d, J = 2.84 Hz, Ar−H), 7.48−7.45 (1H, m, Ar−H), 7.40 (1H, d, J = 8.56 Hz, Ar−H), 7.33 (1H, m, Ar−H), 7.17 (1H, dd, J = 2.64, 8.52 Hz, Ar−H), 6.94 (1H, d, J = 5.32 Hz, Ar−H), 6.65−6.60 (2H, m, Ar−H), 3.67 (2H, s, CH$_2$N), 3.56 (4H, t, J = 4.96 Hz, 2 × CH$_2$N), 2.67 (4H, t, J = 5.12 Hz, 2 × CH$_2$); ^{13}C NMR (100 MHz, CDCl$_3$) δ 159.8, 150.1, 149.5, 148.2, 147.7, 138.4, 137.9, 136.6, 130.9, 130.6, 127.1, 126.7, 125.2, 122.9, 122.8, 118.2, 113.7, 107.5, 102.3, 59.3, 51.0, 45.6; MS (ES−) m/z 462 ([M − H]$^-$, 100), 464 (50), 466 (4); HRMS m/z 462.1258 (C$_{25}$H$_{22}$^{35}Cl$_2$N$_5$ requires 462.1252). Anal. (C, H, N).

[4-Chloro-3-(4-isopropylpiperazin-1-ylmethyl)phenyl](7-chloroquinolin-4-yl)amine (3m). Yellow solid (0.31 g, 61%); ^{1}H (400 MHz, MeOD) δ 8.43 (1H, d, J = 5.53 Hz, Ar−H), 8.29 (1H, d, J = 9.03, Ar−H), 7.89 (1H, d, J = 2.05 Hz, Ar−H), 7.53 (1H, dd, J = 2.05, 9.03 Hz, Ar−H), 7.46 (1H, d, J = 8.53 Hz, Ar−H), 7.30 (1H, dd, J = 2.68, 8.53 Hz, Ar−H), 6.98 (2H, d, J = 5.55 Hz, Ar−H), 3.72 (2H, s, CH$_2$), 3.33 (1H, s, CH), 2.82 (4H, bs, 2 × CH$_2$), 2.71 (4H, bs, 2 × CH$_2$), 1.19 (6H, s, (CH$_3$)$_2$); ^{13}C (100 MHz, MeOD) δ 152.9, 151.1, 150.6, 140.8, 138.1, 137.3, 132.0, 131.3, 128.3, 127.4, 126.8, 125.2, 124.8, 120.2, 103.6, 60.1, 57.4, 55.2, 53.5, 18.7; MS (ES−) m/z 427/429/431 ([M − H]$^-$); HRMS m/z 427.1454 (C$_{23}$H$_{25}$^{35}Cl$_2$N$_4$ requires 427.1456). Anal. (C, H, N).

(7-Chloroquinolin-4-yl)(4-chloro-3-imidazol-1-ylmethylphenyl)amine (3n). Yellow solid; 71.9 mg, 33%; ^{1}H (400 MHz, MeOD) δ 8.43 (1H, d, J = 5.83 Hz, Ar−H), 8.30 (1H, d, J = 9.06 Hz, Ar−H), 7.91 (1H, d, J = 2.09 Hz, Ar−H), 7.85 (1H, s, Ar−H), 7.58 (1H, dd, J = 2.09, 9.06 Hz, Ar−H), 7.56 (1H, d, J = 8.54 Hz), 7.40 (1H, dd, J = 2.66 Hz, 8.54 Hz, Ar−H), 7.22 (1H, s, Ar−H), 7.12 (1H, d, J = 2.47 Hz, Ar−H), 7.06 (1H, s, Ar−H), 6.94 (1H, d, J = 5.83 Hz, Ar−H), 4.81 (2H, s, CH$_2$); ^{13}C (100 MHz, MeOD) δ 150.3,

147.7, 144.5, 138.4, 138.3, 135.8, 130.8, 130.2, 129.5, 126.7, 125.4, 124.8, 124.6, 122.4, 121.5, 118.7, 113.5, 103.2, 46.0; MS (CI) *m/z* 369 ([M + H]$^+$, 100), 371 (67), 373 (15); HRMS *m/z* 369.067 94 (C$_{19}$H$_{15}$Cl$_2$N$_4$ requires 369.067 38). Anal. (C, H, N).

[3-(*tert*-Butylaminomethyl)phenyl](7-chloroquinolin-4-yl)amine (6f). Preparation according to general procedure 3, using **6d**, gave **6f** as a yellow solid after purification by column chromatography (20% MeOH in CH$_2$Cl$_2$): 0.89 g, 39%; ^{1}H (400 MHz, MeOD) δ 8.64 (1H, d, *J* = 9.12 Hz, Ar−H), 8.45 (1H, d, *J* = 7.06 Hz, Ar−H), 8.01 (1H, d, *J* = 1.96 Hz, Ar−H), 7.73 (1H, dd, *J* = 1.96, 9.12 Hz, Ar−H), 7.75−7.73 (2H, m, Ar−H), 7.65−7.57 (2H, m, Ar−H), 7.03 (1H, d, *J* = 7.04 Hz, Ar−H), 3.33 (2H, s, CH$_2$), 1.53 (9H, s, (CH$_3$)$_3$); ^{13}C (100 MHz, CDCl$_3$) δ 150.1, 148.0, 145.5, 138.1, 135.8, 130.3, 129.8, 129.5, 126.7, 121.9, 118.8, 115.2, 114.9, 113.5, 103.6, 51.2, 46.9, 29.8, 29.5; MS (CI) *m/z* 340 ([M + H]$^+$, 100); HRMS *m/z* 340.157 29 (C$_{20}$H$_{23}$ClN$_3$requires 340.158 02). Anal. (C, H, N).

(7-Chloroquinolin-4-yl)(3-imidazol-1-ylmethylphenyl)amine (6g). Preparation according to general procedure 3, using **6e**, gave **6g** as a yellow solid after purification by column chromatography (5% MeOH in CH$_2$Cl$_2$): 162 mg, 25%; ^{1}H (400 MHz, MeOD) δ 8.35 (1H, d, *J* = 5.50 Hz, Ar−H), 8.22 (1H, d, *J* = 9.06), 7.84 (1H, d, *J* = 2.09 Hz, Ar−H), 7.77 (1H, s, Ar−H), 7.44 (1H, dd, *J* = 2.09 Hz, 9.06 Hz, Ar−H), 7.42 (1H, t, *J* = 7.79 Hz, Ar−H), 7.32 (1H, d, *J* = 7.97 Hz, Ar−H), 7.22 (1H, t, *J* = 1.71 Hz, Ar−H), 7.15 (1H, t, *J* = 1.33, Ar−H), 7.09 (1H, dd, *J* = 0.57 Hz, 7.59 Hz, Ar−H), 7.02 (1H, t, *J* = 1.14 Hz, Ar−H), 6.90 (1H, d, *J* = 5.50 Hz, Ar−H), 4.86 (2H, s, CH$_2$); ^{13}C (100 MHz, MeOD) δ 152.8, 151.2, 150.9, 142.4, 140.5, 139.1, 137.2, 131.6, 129.9, 128.2, 127.2, 125.3, 125.1, 124.2, 123.5, 121.4, 120.3, 103.4, 51.8; MS (CI) *m/z* 335 ([M + H]$^+$, 70), 337 (30), 339 (3), 301 (56); HRMS *m/z* 335.105 68 (C$_{19}$H$_{16}$ClN$_4$requires 335.106 32). Anal. (C, H, N).

Antimalarial Activity. Parasites were maintained in culture according to previously published work.[22] In vitro antimalarial activity was assessed using the methods described by Smilkstein.[24] For this assay, after 48 h of growth, 100 μL of SYBR Green I in lysis buffer (0.2 μL of SYBR Green I/mL of lysis buffer) was added to each well, and the contents were mixed until no visible erythrocyte sediment remained. After 1 h of incubation in the dark at room temperature, fluorescence was measured using a Thermo Electron Corporation VARIOSKAN fluorescent plate reader, with excitation and emission wavelength bands centered at 485 and 530 nm, respectively, and processed using the Thermo SkanIt RE proprietry software package. The background reading for an empty well was subtracted to yield fluorescence counts for analysis. Analysis of the counts obtained by both assay methods was performed with the Grafit data analysis and graphics program (Erithacus software, version 3.01). The counts were plotted against the logarithm of the drug concentration and curve fitting was done by nonlinear regression (sigmoidal dose-response/variable slope equation) to yield the drug concentration that produced 50% of the observed decline from the maximum counts in the drug-free control wells (IC$_{50}$).

In Vivo Antimalarial Activity. The efficacy of selected 4-aminoquinolines was measured against *P. yoelii* or *P. berghei* in a "4-day test" (Peters et al.).[28] Cohorts of age-matched female CD1 mice were infected iv with 6.4 × 10^6 or 10.0 × 10^6 parasites obtained from infected donors, and the mice were randomly distributed in groups of *n* = 5 mice/group (day 0). Treatments were administered from day 0 (1 h after infection) until day 3. The percentage of YOYO-1+ murine erythrocytes in peripheral blood at day 4 after infection was measured (*Cytometry, Part A*, **2005**, *67*, 27−36) and recrudescence up to days 22−25 if the parasitemias were below our detection limit (0.01%) at day 4 after infection. The therapeutic efficacy of compounds was expressed as the effective dose (mg·kg/ (body weight)) that reduces parasitemia by 50% (ED$_{50}$) and 90% (ED$_{90}$) with respect to vehicle treated groups (ED$_{90}$) and the dose that achieved eradication of parasitemia until day 23 after infection (NRL). All compounds and corresponding vehicles were administered orally at 20 mg·kg^{-1} or subcutaneously at 10 mg·kg^{-1}, as

appropriate. Chloroquine or amodiaquine was included as assay quality control for each in vivo assay of *P. yoelii* or *P. berghei*, respectively.

Disposition and Metabolism Studies on 2k and 3k. Materials. [^{3}H]**2k** (24.08 Ci/mmol; radiochemical purity by HPLC greater than 97%) and [^{3}H]**3k** (46.50 Ci/mmol; radiochemical purity by HPLC greater than 98%) were prepared from [^{3}H]4,7-dichloroquinoline (general method 1a). Tissue solubilizer-450 (0.5 N quaternary ammonium hydroxide in toluene) was purchased from Beckmann Chemicals (Bremen, Germany). Ultima Flo and Ultima Gold scintillant were from Packard Bioscience BV (Groningen, The Netherlands). HPLC grade solvents were products of Fisher Scientific (Loughborough, Leicestershire, U.K.).

Adult male Wistar rats (200−400 g) were obtained from Charles River (Margate, U.K.). The protocols described were undertaken in accordance with criteria outlined in a license granted under the Animals (Scientific Procedures) Act of 1986 and approved by the University of Liverpool Animal Ethics Committee.

Methods. In Vivo Metabolism of [^{3}H]2k and [^{3}H]3k in the Rat (5 h). Adult male Wistar rats (250−400 g, *n* = 4) were anesthetized with urethane (1.4 g/mL in isotonic saline; 1 mL/kg, ip). Polyethylene cannulae were inserted into the trachea, femoral vein, and common bile duct, and the penis was ligated. Drug-blank bile was collected for approximately 20 min before treatment. [^{3}H]**2k** or [^{3}H]**3k** (54 μmol/kg, 20 μCi/rat) was dissolved in saline (0.5−1 mL depending on animal weight) and was injected over 10 min (iv). Bile was collected hourly for a time period of 5 h into preweighed Eppendorf tubes. Samples were weighed after collection to determine the extent of biliary secretion and stored at −30 °C until analysis by LC−MS.

After 5 h, urine was aspirated from the bladder and transferred to a preweighed Eppendorf tube and a cardiac puncture was performed. The blood was centrifuged (1000*g*, 6 min) and the plasma transferred to a separate tube. The plasma from each experiment was pooled together, and then blood proteins were removed by the exhaustive addition of MeOH (5 equiv) followed by centrifugation (1200*g*, 10 min). The supernatant was removed and concentrated by evaporation before redissolving it in MeOH (200 μL). The plasma and urine samples were stored at −30 °C until analysis by LC−MS. Aliquots of bile and urine (30 μL) were mixed with scintillant (4 mL) for determination of radioactivity.

LC−MS Analysis of Bile, Urine, and Plasma Samples. Aliquots of bile, urine, and plasma (100 μL) were analyzed at room temperature on a Hypersil 5-μm HyPurity Elite C-18 column (150 mm × 4.6 mm; Thermo Hypersil-Keystone, Runcorn, Cheshire, U.K.) with a gradient of acetonitrile (10−50% over 30 min (**2k**), 20−50% over 30 min (**3k**)) in trifluoroacetic acid (0.1%, v/v). The LC system consisted of two Jasco PU980 pumps (Jasco UK, Great Dunmow, Essex, U.K.) and a Jasco HG-980-30 mixing module. The flow rate was 0.9 mL/min. Eluate split-flow to the LC−MS interface was ∼40 μL/min. A Quattro II mass spectrometer (Micromass MS Technologies, Manchester, U.K.) fitted with the standard coaxial electrospray source was used in the positive-ion mode. Nitrogen was used as the nebulizing and drying gas. The interface temperature was 80 °C; the capillary voltage was 3.9 kV. Spectra were acquired between *m/z* 100 and 1050 over a scan duration of 5 s. Fragmentation of analyte ions was achieved at a cone voltage of 50−70 V. Data were processed with MassLynx 3.5 software (Micromass). Radiolabeled analytes in the remainder of the eluate were detected with a Radiomatic A250 flow detector (Packard, Pangbourne, Berkshire, U.K.). Eluate was mixed with Ultima-Flo AP scintillant (Packard Bioscience BV, Groningen, The Netherlands) at 1 mL/min.

In Vivo Retention Studies of [^{3}H]2k and [^{3}H]3k in the Rat. Adult male Wistar rats (200−400 g, *n* = 4) were administered a solution of [^{3}H]**2k** or [^{3}H]**3k** (54 μmol/kg, 20 μCi/rat) dissolved in saline (0.5−1 mL, ip). The animals were then transferred to individual metabolism cages equipped with a well for collecting urine and faeces. The rats were allowed food and drink ad libitum for a 24 h period before administration of a lethal dose of pentabarbitone.

Aliquots of urine (30 μL) were collected and mixed with scintillant for determination of radioactivity. The collected feces were weighed and dissolved in distilled water for a period of 16 h before determination of radioactivity. The major organs were then removed and assessed for radioactivity.

In Vivo Retention Studies of [³H]2k and [³H]3k in the Rat (48 h). Adult male Wistar rats ($n = 4$) were administered a solution of either [³H]**2k** or [³H]**3k** (54 μmol/kg, 20 μCi/rat) dissolved in saline (0.5−1 mL, ip). The animals were kept in a normal animal cage for a period of 24 h before they were transferred to individual metabolism cages equipped with a well for collecting urine and faeces. The rats remained in the metabolism cages for a further 24 h, with full access to food and drink, before overdose using pentabarbitone.

Aliquots of urine (30 μL) were collected and mixed with scintillant for determination of radioactivity. The collected feces were weighed and dissolved in distilled water for a period of 16 h before determination of radioactivity). The major organs were then removed and assessed for radioactivity.

In Vivo Retention Studies of [³H]2k and [³H]3k in the Rat (168−240 h). Adult male Wistar rats ($n = 4$) were administered a solution of [³H]**2k** or [³H]**3k** (54 μmol/kg, 20 μCi/rat) dissolved in saline (0.5−1 mL, ip). The animals were kept in a normal animal cage for a period of 168 or 240 h with full access to food and drink before administration of a lethal dose of pentabarbitone. The major organs were then removed and assessed for radioactivity.

Tissue Distribution of [³H]2k and [³H]3k in the Rat. At the end of the relevant time point (5, 24, 48, 168, or 240 h) the animals were killed by a lethal dose of pentabarbitone and the major organs were excised (brain, eyes, heart, lungs, liver, kidneys, spleen, testes, and skin) and stored at −30 °C. Duplicate portions (50−100 mg) of the tissues and feces were weighed and solubilized in tissue solubilizer (0.75 mL) at 50 °C for 16 h. The solutions were decolorized with hydrogen peroxide (200 μL) over 1 h and then neutralized using glacial acetic acid (30 μL) before leaving in the darkness for 16 h to prevent chemoluminescence. Ultima Gold scintillant (10 mL) was added before the radioactivity was determined by scintillation counting.

Cytotoxicity of 2k and 3f in Isolated Rat Hepatocytes. Male Wistar rats (200−250 g) ($n = 3$) were terminally anesthetised with pentobarbitone sodium (90 mg/kg in isotonic saline ip). Hepatocytes were isolated using a two-step collagenase perfusion method adapted from that of Guguen-Guillouzo.[55] The abdomen was opened and the liver cannulated through the portal vein using a gauge catheter. Before perfusion, the heart was removed to allow free loss of perfusion buffers. The liver was washed with calcium-free HEPES buffer for 10 min at a flow rate of 40 mL/min. The liver was then perfused with digestion buffer, a mixture of wash buffer with 5% CaCl$_2$ solution, for 6−10 min. The digested tissue was then excised and placed in a Petri dish containing wash buffer and DNAase (0.1% w/v). The tissue was anchored, and the Glison's capsule was disrupted and disturbed to release the cells. The cell suspension was filtered through gauze to eliminate cell debris, blood, and sinusoidal cells. The cells were washed three times in DNAase wash buffer before resuspending in incubation buffer (HEPES buffer and MgSO$_4$·7H$_2$0 (0.25% w/v)). Cell viability was then assessed microscopically using the trypan blue exclusion test. The cells were then incubated with various concentrations of the relevant compound for a period of 6 h before determining cell viability in the presence of test compound using the trypan blue exclusion test and MTS assay.

Statistical Analysis. All results are expressed as the mean ± standard error of the mean (SEM). Values to be compared were analyzed for non-normality using the Shapiro−Wilk test. Student t tests were used when normality was indicated. A Mann−Whitney U test was used for nonparametric data. For analysis of sets of data with variance, a one-way analysis of variance (ANOVA) test was used for parametric data and a Kruskell−Wallis test was used for nonparametric data. All calculations were performed using StatsDirect statistical software, and results were considered to be significant when $P < 0.05$.

Supporting Information Available: Synthetic procedures and characterization data for intermediates, procedures for equilibrium binding studies, metabolism and disposition studies, and protocols for pharmacokinetics/safety evaluation. This material is available free of charge via the Internet at http://pubs.acs.org.

References

(1) White, N. J.; Nosten, F.; Looareesuwan, S.; Watkins, W. M.; Marsh, K.; Snow, R. W.; Kokwaro, G.; Ouma, J.; Hien, T. T.; Molyneux, M. E.; Taylor, T. E.; Newbold, C. I.; Ruebush, T. K.; Danis, M.; Greenwood, B. M.; Anderson, R. M.; Olliaro, P. Averting a malaria disaster. *Lancet* **1999**, *353*, 1965–1967.

(2) Greenwood, B. M.; Fidock, D. A.; Kyle, D. E.; Kappe, S. H. I.; Alonso, P. L.; Collins, F. H.; Duffy, P. E. Malaria: progress, perils, and prospects for eradication. *J. Clin. Invest.* **2008**, *118*, 1266–1276.

(3) Tilley, L.; Davis, T. M. E.; Bray, P. G. Prospects for the treatment of drug-resistant malaria parasites. *Future Microbiol.* **2006**, *1*, 127–141.

(4) Kelly-Hope, L.; Ranson, H.; Hemingway, J. Lessons from the past: managing insecticide resistance in malaria control and eradication programmes. *Lancet Infect. Dis.* **2008**, *8*, 387–389.

(5) Goldberg, D. E. Plasmodial hemoglobin degradation: an ordered pathway in a specialized organelle. *Infect. Agents Dis.* **1992**, *1*, 207–211.

(6) Francis, S. E.; Sullivan, D. J.; Goldberg, D. E. Hemoglobin metabolism in the malaria parasite *Plasmodium falciparum*. *Annu. Rev. Microbiol.* **1997**, *51*, 97–123.

(7) Mungthin, M.; Bray, P. G.; Ridley, R. G.; Ward, S. A. Central role of hemoglobin degradation in mechanisms of action of 4-aminoquinolines, quinoline methanols, and phenanthrene methanols. *Antimicrob. Agents Chemother.* **1998**, *42*, 2973–2977.

(8) Bray, P. G.; Mungthin, M.; Ridley, R. G.; Ward, S. A. Access to hematin: the basis of chloroquine resistance. *Mol. Pharmacol.* **1998**, *54*, 170–179.

(9) O'Neill, P. M.; Bray, P. G.; Hawley, S. R.; Ward, S. A.; Park, B. K. 4-Aminoquinolines. Past, present, and future: a chemical perspective. *Pharmacol. Ther.* **1998**, *77*, 29–58.

(10) Hawley, S. R.; Bray, P. G.; Mungthin, M.; Atkinson, J. D.; O'Neill, P. M.; Ward, S. A. Relationship between antimalarial drug activity, accumulation, and inhibition of heme polymerization in *Plasmodium falciparum* in vitro. *Antimicrob. Agents Chemother.* **1998**, *42*, 682–686.

(11) Bray, P. G.; Martin, R. E.; Tilley, L.; Ward, S. A.; Kirk, K.; Fidock, D. A. Defining the role of PfCRT in *Plasmodium falciparum* chloroquine resistance. *Mol. Microbiol.* **2005**, *56*, 323–333.

(12) Hawley, S. R.; Bray, P. G.; Park, B. K.; Ward, S. A. Amodiaquine accumulation in *Plasmodium falciparum* as a possible explanation for its superior antimalarial activity over chloroquine. *Mol. Biochem. Parasitol.* **1996**, *80*, 15–25.

(13) (a) Neftel, K. A.; Woodtly, W.; Schmid, M.; Frick, P. G.; Fehr, J. Amodiaquine induced agranulocytosis and liver-damage. *Br. Med. J.* **1986**, *292*, 721–723. (b) Although there are toxicity concerns with amodiaquine, a new combination of artesunate and amodiaquine (ASAQ) has been launched and amodiaquine continues to be used for uncomplicated malaria in many African countried in combination with sulfadoxine/pyrimethamine.

(14) Schulthess, H. K.; von Felten, A.; Gmur, J.; Neftel, K. Amodiaquine-induced agranulocytosis during suppressive treatment of malaria—demonstration of an amodiaquine-dependent granulocytotoxic antibody. *Schweiz. Med. Wochenschr.* **1983**, *113*, 1912–1913.

(15) Maggs, J. L.; Tingle, M. D.; Kitteringham, N. R.; Park, B. K. Drug−protein conjugates. 14. Mechanisms of formation of protein-arylating intermediates from amodiaquine, a myelotoxin and hepatotoxin in man. *Biochem. Pharmacol.* **1988**, *37*, 303–311.

(16) Maggs, J. L.; Park, B. K. Cyto-toxicity of the quinoneimine of amodiaquine. *Br. J. Clin. Pharmacol.* **1988**, *25*, P143.

(17) Maggs, J. L.; Colbert, J.; Winstanley, P. A.; Orme, M. L.; Park, B. K. Irreversible binding of amodiaquine to human-liver microsomes: chemical and metabolic factors. *Br. J. Clin. Pharmacol.* **1987**, *23*, P649.

(18) Harrison, A. C.; Kitteringham, N. R.; Clarke, J. B.; Park, B. K. The mechanism of bioactivation and antigen formation of amodiaquine in the rat. *Biochem. Pharmacol.* **1992**, *43*, 1421–1430.

(19) Rouveix, B.; Coulombel, L.; Aymard, J. P.; Chau, F.; Abel, L. Amodiaquine-induced immune agranulocytosis. *Br. J. Clin. Haematol.* **1989**, *71*, 7–11.

(20) Clarke, J. B.; Neftel, K.; Kitteringham, N. R.; Park, B. K. Detection of antidrug IgG antibodies in patients with adverse drug-reactions to amodiaquine. *Int. Arch. Allergy Appl. Immunol.* **1991**, *95*, 369–375.

(21) O'Neill, P. M.; Harrison, A. C.; Storr, R. C.; Hawley, S. R.; Ward, S. A.; Park, B. K. The effect of fluorine substitution on the metabolism and antimalarial activity of amodiaquine. *J. Med. Chem.* **1994**, *37*, 1362–1370.

(22) O'Neill, P. M.; Mukhtar, A.; Stocks, P. A.; Randle, L. E.; Hindley, S.; Ward, S. A.; Storr, R. C.; Bickley, J. F.; O'Neil, I. A.; Maggs, J. L.; Hughes, R. H.; Winstanley, P. A.; Bray, P. G.; Park, B. K. Isoquine and related amodiaquine analogues: a new generation of improved 4-aminoquinoline antimalarials. *J. Med. Chem.* **2003**, *46*, 4933–4945.

(23) Lawrence, R. M.; Dennis, K. C.; O'Neill, P. M.; Hahn, D. U.; Roeder, M.; Struppe, C. Development of a scalable synthetic route to GSK369796 (*N-tert*-butyl isoquine), a novel 4-aminoquinoline antimalarial drug. *Org. Process Res. Dev.* **2008**, *12*, 294–297.

(24) Smilkstein, M.; Sriwilaijaroen, N.; Kelly, J. X.; Wilairat, P.; Riscoe, M. Simple and inexpensive fluorescence-based technique for high-throughput antimalarial drug screening. *Antimicrob. Agents Chemother.* **2004**, *48*, 1803–1806.

(25) Trager, W.; Jenson, J. B. Cultivation of malarial parasites. *Nature* **1978**, *273*, 621–622.

(26) Stocks, P. A.; Raynes, K. J.; Bray, P. G.; Park, B. K.; O'Neill, P. M.; Ward, S. A. Novel short chain chloroquine analogues retain activity against chloroquine resistant K1 *Plasmodium falciparum*. *J. Med. Chem.* **2002**, *45*, 4975–4983.

(27) Gemma, S.; Campiani, G.; Butini, S.; Kukreja, G.; Coccone, S. S.; Joshi, B. P.; Persico, M.; Nacci, V.; Fiorini, I.; Novellino, E.; Fattorusso, E.; Taglialatela-Scafati, O.; Savini, L.; Taramelli, D.; Basilico, N.; Parapini, S.; Morace, G.; Yardley, V.; Croft, S.; Coletta, M.; Marini, S.; Fattorusso, C. Clotrimazole scaffold as an innovative pharmacophore towards potent antimalarial agents: design, synthesis, and biological and structure–activity relationship studies. *J. Med. Chem.* **2008**, *51*, 1278–1294.

(28) Peters, W.; Robinson, B. L. *Handbook of Animal Models of Infection*; Academic Press: San Diego, CA, 1999; pp 757–773.

(29) Vippagunta, S. R.; Dorn, A.; Ridley, R. G.; Vennerstrom, J. L. Characterization of chloroquine–hematin mu-oxo dimer binding by isothermal titration calorimetry. *Biochim. Biophys. Acta* **2000**, *1475*, 133–140.

(30) Dorn, A.; Vippagunta, S. R.; Matile, H.; Jaquet, C.; Vennerstrom, J. L.; Ridley, R. G. An assessment of drug–haematin binding as a mechanism for inhibition of haematin polymerisation by quinoline antimalarials. *Biochem. Pharmacol.* **1998**, *55*, 727–736.

(31) Vippagunta, S. R.; Dorn, A.; Matile, H.; Bhattacharjee, A. K.; Karle, J. M.; Ellis, W. Y.; Ridley, R. G.; Vennerstrom, J. L. Structural specificity of chloroquine–hematin binding related to inhibition of hematin polymerization and parasite growth. *J. Med. Chem.* **1999**, *42*, 4630–4639.

(32) Egan, T. J. Haemozoin formation. *Mol. Biochem. Parasitol.* **2008**, *157*, 127–136.

(33) Egan, T. J. Recent advances in understanding the mechanism of hemozoin (malaria pigment) formation. *J. Inorg. Biochem.* **2008**, *102*, 1288–1299.

(34) Egan, T. J.; Ncokazi, K. K. Effects of solvent composition and ionic strength on the interaction of quinoline antimalarials with ferriprotoporphyrin IX. *J. Inorg. Biochem.* **2004**, *98*, 144–152.

(35) Egan, T. J.; Mavuso, W. W.; Ross, D. C.; Marques, H. M. Thermodynamic factors controlling the interaction of quinoline antimalarial drugs with ferriprotoporphyrin IX. *J. Inorg. Biochem.* **1997**, *68*, 137–145.

(36) Casabianca, L. B.; An, D.; Natarajan, J. K.; Alumasa, J. N.; Roepe, P. D.; Wolf, C.; de Dios, A. C. Quinine and chloroquine differentially perturb heme monomer–dimer equilibrium. *Inorg. Chem.* **2008**, *47*, 6077–6081.

(37) Parapini, S.; Basilico, N.; Pasini, E.; Egan, T. J.; Olliaro, P.; Taramelli, D.; Monti, D. Standardization of the physicochemical parameters to assess in vitro the beta-hematin inhibitory activity of antimalarial drugs. *Exp. Parasitol.* **2000**, *96*, 249–256.

(38) Oda, Y.; Funasaka, K.; Kitano, M.; Nakama, A.; Yoshikura, T. Use of a high-throughput umu-microplate test system for rapid detection of genotoxicity produced by mutagenic carcinogens and airborne particulate matter. *Environ. Mol. Mutagen.* **2004**, *43*, 10–19.

(39) Davis, T. M. E.; Hung, T. Y.; Sim, I. K.; Karunajeewa, H. A.; Ilett, K. F. Piperaquine: a resurgent antimalarial drug. *Drugs* **2005**, *65*, 75–87.

(40) Hien, T. T.; Dolecek, C.; Mai, P. P.; Dung, N. T.; Truong, N. T.; Thai, L. H.; An, D. T. H.; Thanh, T. T.; Stepniewska, K.; White, N. J.; Farrar, J. Dihydroartemisinin–piperaquine against multidrug-resistant *Plasmodium falciparum* malaria in Vietnam: randomised clinical trial. *Lancet* **2004**, *363*, 18–22.

(41) Chen, L.; Qu, F.; Zhou, Y. Field observations on the antimalarial piperaquine. *Chin. Med. J.* **1982**, *95*, 281–286.

(42) Price, R. N.; Hasugian, A. R.; Ratcliff, A.; Siswantoro, H.; Purba, H. L. E.; Kenangalem, E.; Lindegardh, N.; Penttinen, P.; Laihad, F.; Ebsworth, E. P.; Anstey, N. M.; Tjitra, E. Clinical and pharmacological determinants of the therapeutic response to dihydroartemisinin–piperaquine for drug-resistant malaria. *Antimicrob. Agents Chemother.* **2007**, *51*, 4090–4097.

(43) Khanh, N. X.; de Vries, P. J.; Ha, L. D.; van Boxtel, C. J.; Koopmans, R.; Kager, P. A. Declining concentrations of dihydroartemisinin in plasma during 5-day oral treatment with artesunate for falciparum malaria. *Antimicrob. Agents Chemother.* **1999**, *43*, 690–692.

(44) Delarue, S.; Girault, S.; Maes, L.; Debreu-Fontaine, M. A.; Labaeid, M.; Grellier, P.; Sergheraert, C. Synthesis and in vitro and in vivo antimalarial activity of new 4-anilinoquinolines. *J. Med. Chem.* **2001**, *44*, 2827–2833.

(45) Miroshnikova, O. V.; Hudson, T. H.; Gerena, L.; Kyle, D. E.; Lin, A. J. Synthesis and antimalarial activity of new isotebuquine analogues. *J. Med. Chem.* **2007**, *50*, 889–896.

(46) Casagrande, M.; Basilico, N.; Parapini, S.; Romeo, S.; Taramelli, D.; Sparatore, A. Novel amodiaquine congeners as potent antimalarial agents. *Bioorg. Med. Chem.* **2008**, *16*, 6813–6823.

(47) Mzayek, F.; Deng, H. Y.; Mather, F. J.; Wasilevich, E. C.; Liu, H. Y.; Hadi, C. M.; Chansolme, D. H.; Murphy, H. A.; Melek, B. H.; Tenaglia, A. N.; Mushatt, D. M.; Dreisbach, A. W.; Lertora, J. J. L.; Krogstad, D. J. Randomized dose-ranging controlled trial of AQ-13, a candidate antimalarial, and chloroquine in healthy volunteers. *PloS Clin. Trials* **2007**, *2*, e6.

(48) Dive, D. Ferrocene conjugates of chloroquine and other antimalarials: the development of ferroquine, a new antimalarial. *ChemMedChem* **2008**, *3*, 383–391.

(49) Warhurst, D. C.; Craig, J. C.; Adagu, P. S.; Guy, R. K.; Madrid, P. B.; Fivelman, Q. L. Activity of piperaquine and other 4-aminoquinoline antiplasmodial drugs against chloroquine-sensitive and resistant blood-stages of *Plasmodium falciparum*: role of beta-haematin inhibition and drug concentration in vacuolar water- and lipid-phases. *Biochem. Pharmacol.* **2007**, *73*, 1910–1926.

(50) Kuhn, Y.; Rohrbach, P.; Lanzer, M. Quantitative pH measurements in *Plasmodium falciparum*-infected erythrocytes using pHluorin. *Cell. Microbiol.* **2007**, *9*, 1004–1013.

(51) Pisciotta, J. Neutral lipid microspheres in *Plasmodium falciparum* digestive vacuoles mediate heme crystallization. *Am. J. Trop. Med. Hyg.* **2005**, *73*, 188.

(52) Pisciotta, J. M.; Coppens, I.; Tripathi, A. K.; Scholl, P. F.; Shuman, J.; Bajad, S.; Shulaev, V.; Sullivan, D. J., Jr. The role of neutral lipid nanospheres in *Plasmodium falciparum* haem crystallization. *Biochem. J.* **2007**, *402*, 197–204.

(53) Tetko, I. V.; Gasteiger, J.; Todeschini, R.; Mauri, A.; Livingstone, D.; Ertl, P.; Palyulin, V. A.; Radchenko, E. V.; Zefirov, N. S.; Makarenko, A. S.; Tanchuk, V. Y.; Prokopenko, V. V. Virtual computational chemistry laboratory: design and description. *J. Comput.-Aided Mol. Des.* **2005**, *19*, 453–463.

(54) Wennerholm, A.; Nordmark, A.; Pihlsgard, M.; Mahindi, M.; Bertilsson, L.; Gustafsson, L. L. Amodiaquine, its desethylated metabolite, or both, inhibit the metabolism of debrisoquine (CYP2D6) and losartan (CYP2C9) in vivo. *Eur. J. Clin. Pharmacol.* **2006**, *62*, 539–546.

(55) Guguen-Guillouzo, C.; Guillouso, A. Methods for Preparation of Adult and Fetal Hepatocytes. In *Research in Isolated and Cultured Hepatocytes*; Guillouzo, A., Guguen-Guillouzo, C., Eds.; John Libbey Eurotext/INSERM: London/Paris, 1986; pp 1–12.